

SUPERSYMMETRIC DARK MATTER, INFLATION AND YUKAWA QUASI-UNIFICATION

G. LAZARIDES AND C. PALLIS

*Physics Division, School of Technology,
Aristotle University of Thessaloniki,
54124 Thessaloniki, GREECE
lazaride@eng.auth.gr, kpallis@auth.gr*

February 2, 2008

Abstract

The construction of specific supersymmetric grand unified models based on the Pati-Salam gauge group and leading to a set of Yukawa quasi-unification conditions is briefly reviewed. For each sign of the parameter μ , an appropriately chosen condition from this set can allow an acceptable b -quark mass within the constrained minimal supersymmetric standard model. The restrictions on the parameter space which arise from the cold dark matter constraint, the inclusive decay $b \rightarrow s\gamma$, the muon anomalous magnetic moment and the collider bounds are also investigated. For $\mu > 0$, a wide and natural range of parameters is allowed. On the contrary, the $\mu < 0$ case not only is disfavored by the present experimental data on the muon anomalous magnetic moment, but also is excluded by the combination of the cold dark matter and $b \rightarrow s\gamma$ requirements. In the $\mu > 0$ case, the predicted neutralinos are possibly detectable in the future direct cold dark matter searches. Moreover, the μ term is generated via a Peccei-Quinn symmetry and proton is practically stable. The same model gives rise to a new shifted inflationary scenario, which is based only on renormalizable terms, does not suffer from the problem of monopole overproduction at the end of inflation and is compatible with the cosmic microwave background radiation constraint. Although the relevant part of inflation takes place at values of the inflaton field which are not much smaller than the reduced Planck scale and, thus, supergravity corrections could easily invalidate inflation, this does not happen provided that an extra gauge singlet with a superheavy vacuum expectation value, which originates from D-terms, is introduced and a specific form of the Kähler potential is used. The constraint from the cosmic background explorer can again be met by readjusting the values of the parameters which were obtained with global supersymmetry.

1 Introduction

The constrained minimal supersymmetric standard model (CMSSM), which is a highly predictive version of the minimal supersymmetric standard model (MSSM) based on universal boundary conditions [1], can be further restricted by being embedded in a supersymmetric (SUSY) grand unified theory (GUT) with a gauge group containing $SU(4)_c$ and $SU(2)_R$. This can lead [2] to ‘asymptotic’ Yukawa unification (YU) [3], i.e. the exact unification of the third generation Yukawa coupling constants at the SUSY GUT scale M_{GUT} . Indeed, assuming that the electroweak Higgs superfields H_1 , H_2 and the third family right handed quark superfields t^c , b^c form $SU(2)_R$ doublets, we obtain [2] the asymptotic Yukawa coupling relation $h_t = h_b$ and, hence, large $\tan \beta \sim m_t/m_b$. Moreover, if the third generation quark and lepton $SU(2)_L$ doublets [singlets] q_3 and l_3 [b^c and τ^c] form a $SU(4)_c$ 4-plet [$\bar{4}$ -plet] and the Higgs doublet H_1 which couples to them is a $SU(4)_c$ singlet, we get $h_b = h_\tau$ and the asymptotic relation $m_b = m_\tau$ follows. The simplest GUT gauge group which contains both $SU(4)_c$ and $SU(2)_R$ is the Pati-Salam (PS) group $G_{\text{PS}} = SU(4)_c \times SU(2)_L \times SU(2)_R$ (for YU within $SO(10)$, see Ref. [4]).

However, given the experimental values of the top-quark and tau-lepton masses (which, combined with YU, naturally restrict $\tan \beta \sim 50$), the CMSSM supplemented by the assumption of YU yields unacceptable values of the b -quark mass for both signs of the parameter μ . This is due to the generation of sizeable SUSY corrections [5] to m_b (about 20%), which arise from sbottom-gluino (mainly) and stop-chargino loops [5, 6, 7] and have the sign of μ (with the standard sign convention of Ref. [8]). The predicted tree-level $m_b(M_Z)$, which turns out to be close to the upper edge of its 95% confidence level (c.l.) experimental range

$$2.684 \text{ GeV} \lesssim m_b(M_Z) \lesssim 3.092 \text{ GeV} \quad (\text{with } \alpha_s(M_Z) = 0.1185), \quad (1)$$

receives, for $\mu > 0$ [$\mu < 0$], large positive [negative] corrections which drive it well above [a little below] the allowed range. This range is derived [9] from the 95% c.l. range for $m_b(m_b)$ in the \overline{MS} scheme ($3.95 - 4.55$ GeV) [10] evolved up to M_Z in accord with the analysis of Ref. [11]. Consequently, for both signs of μ , YU leads to an unacceptable $m_b(M_Z)$, with the $\mu < 0$ case being much less disfavored.

The usual strategy to resolve this discrepancy is the introduction of several kinds of nonuniversalities in the scalar [12, 13, 14] and/or gaugino [15, 16] sector of MSSM with an approximate preservation of YU. On the contrary, in Ref. [9], this problem is addressed in the context of the PS GUT, without need of invoking departure from the CMSSM universality. The Higgs sector of the model is extended by including an extra $SU(4)_c$ non-singlet Higgs superfield with Yukawa couplings to the quarks and leptons. The Higgs $SU(2)_L$ doublets contained in this superfield can naturally develop [17] subdominant vacuum expectation values (VEVs) and mix with the main electroweak doublets which are assumed to be $SU(4)_c$ singlets and form a $SU(2)_R$ doublet. This mixing can, in general, violate $SU(2)_R$. Consequently, the resulting

electroweak doublets H_1, H_2 do not form a $SU(2)_R$ doublet and break $SU(4)_c$ too. As a consequence, a moderate violation of the YU is obtained, which can allow an acceptable b -quark mass even with universal boundary conditions. Obviously, a small deviation from YU is enough for an acceptable prediction of the b -quark mass when $\mu < 0$, while, for $\mu > 0$, a more pronounced deviation is needed.

In this review, we outline the construction of two particular SUSY GUT models which can cause a deviation from YU adequate for $\mu > 0$ [$\mu < 0$] in the first [second] model. We then discuss the resulting CMSSM in each case and the various astrophysical and experimental requirements which restrict its parameter space. They originate from the data on the cold dark matter (CDM) abundance in the universe derived by the Wilkinson microwave anisotropy probe (WMAP) [18, 19], the inclusive branching ratio of $b \rightarrow s\gamma$ [20], $\text{BR}(b \rightarrow s\gamma)$, the muon anomalous magnetic moment α_μ [21] and the mass of the lightest Higgs boson m_h [22]. We show that, for $\mu > 0$, our model possesses a wide range of parameters which is consistent with all these constraints. On the contrary, for $\mu < 0$, the upper bound on the mass of the lightest sparticle (LSP) from the CDM abundance in the universe is incompatible with the data on $\text{BR}(b \rightarrow s\gamma)$. Thus, the latter scheme is not viable.

The $\mu > 0$ model possesses a number of other interesting features too. The LSP is possibly detectable in the near future direct CDM searches. The μ problem of MSSM is solved [23] via a Peccei-Quinn (PQ) symmetry [24] which also solves the strong CP problem. Although the baryon (B) and lepton (L) numbers are explicitly violated, the proton lifetime is considerably higher than the present experimental limits. Furthermore, the same model leads to a new shifted hybrid inflationary scenario [25], which avoids monopole overproduction at the end of inflation and reproduces the results on the quadrupole anisotropy of the cosmic microwave background radiation (CMBR) from the cosmic background explorer (COBE) measurements [26]. The relevant part of inflation takes place at values of the inflaton field which are not much smaller than the Planck scale and, thus, supergravity (SUGRA) corrections could easily invalidate it. It is, however, shown that inflation can be kept intact provided that an extra gauge singlet is introduced and a specific form of the Kähler potential is used. Although the SUGRA corrections are sizable, the constraints from COBE can again be met by readjusting the values of the parameters which were obtained with global SUSY.

The construction of the models is briefly reviewed in Sec. 2 and the resulting CMSSM is presented in Sec. 3. The parameter space of the CMSSM is restricted in Sec. 5 taking into account a number of cosmological and phenomenological requirements which are exhibited in Sec. 4. The deviation from YU is estimated in Sec. 6. Issues related to the direct LSP detection are examined in Sec. 7. The resolution of the μ problem of MSSM and the stability of the proton are discussed in Secs. 8 and 9 respectively. The new shifted inflationary scenario is outlined in Sec. 10. Finally, we summarize our conclusions in Sec. 11. Details concerning the evaluation of the neutralino–nucleus cross section are given in Appendix A.

2 The Pati-Salam SUSY GUT Models

2.1 The General Set-up

We focus on a SUSY GUT model based on the PS gauge group $G_{\text{PS}} = SU(4)_c \times SU(2)_L \times SU(2)_R$ described in detail in Ref. [27] (see also Ref. [28]). The representations and the transformation properties under G_{PS} as well as the extra global charges of the various superfields contained in the model are presented in Table 1, which also contains the extra Higgs superfields required for accommodating an adequate violation of YU (see below).

The left handed quark and lepton superfields of the r th generation ($r = 1, 2, 3$) are accommodated in a pair of superfields

$$\tilde{F}_r = \begin{pmatrix} d_r & -u_r \\ d_r & -u_r \\ d_r & -u_r \\ e_r & -\nu_r \end{pmatrix} \quad \text{and} \quad \tilde{F}_r^c = \begin{pmatrix} u_r^c & u_r^c & u_r^c & \nu_r^c \\ d_r^c & d_r^c & d_r^c & e_r^c \end{pmatrix}, \quad (2)$$

where tilde denotes transpose with respect to (w.r.t.) $SU(4)_c$. The gauge symmetry G_{PS} can be spontaneously broken down to the standard model (SM) gauge group (G_{SM}) through the VEVs which the superfields

$$\tilde{H}^c = \begin{pmatrix} u_H^c & u_H^c & u_H^c & \nu_H^c \\ d_H^c & d_H^c & d_H^c & e_H^c \end{pmatrix} \quad \text{and} \quad \tilde{\bar{H}}^c = \begin{pmatrix} \bar{u}_H^c & \bar{d}_H^c \\ \bar{u}_H^c & \bar{d}_H^c \\ \bar{u}_H^c & \bar{d}_H^c \\ \bar{\nu}_H^c & \bar{e}_H^c \end{pmatrix} \quad (3)$$

acquire in their right handed neutrino directions ν_H^c and $\bar{\nu}_H^c$. The model also contains a gauge singlet S which triggers the breaking of G_{PS} , a $SU(4)_c$ **6**-plet G which gives [29] masses to the right handed down quark type components of H^c , \bar{H}^c and a pair of gauge singlets N , \bar{N} for solving [23] the μ problem of the MSSM via a PQ symmetry (see Sec. 8). In addition to G_{PS} , the model possesses two global $U(1)$ symmetries, namely a PQ and a R symmetry, as well as a discrete Z_2^{mp} symmetry ('matter parity') under which F , F^c change sign. Note that global continuous symmetries such as our PQ and R symmetry can effectively arise [30] from the rich discrete symmetry groups encountered in many compactified string theories (see e.g. Ref. [31]).

In the simplest realization of this model [29], the electroweak doublets H_1, H_2 are exclusively contained in the bidoublet superfield h , which can be written as

$$h = \begin{pmatrix} h_2 & h_1 \end{pmatrix} = \begin{pmatrix} h_2^+ & h_1^0 \\ h_2^0 & h_1^- \end{pmatrix}. \quad (4)$$

Under these circumstances, $H_i = h_i$ with $i = 1, 2$ and so the model predicts YU at M_{GUT} (which is determined by the requirement of the unification of the gauge coupling constants), i.e.

$$h_t : h_b : h_\tau = 1 : 1 : 1, \quad (5)$$

SUPER-FIELDS UNDER G_{PS}	REPRESE-NATIONS UNDER G_{PS}	TRASFOR-MATIONS UNDER G_{PS}	GLOBAL CHARGES	R	PQ	Z_2^{mp}
MATTER SUPERFIELDS						
F_r	$(\mathbf{4}, \mathbf{2}, \mathbf{1})$	$F_r U_L^\dagger U_c^\top$	$1/2$	-1	1	
F_r^c	$(\bar{\mathbf{4}}, \mathbf{1}, \mathbf{2})$	$U_c^* U_R^* F_r^c$	$1/2$	0	-1	
HIGGS SUPERFIELDS						
H^c	$(\bar{\mathbf{4}}, \mathbf{1}, \mathbf{2})$	$U_c^* U_R^* H^c$	0	0	0	
\bar{H}^c	$(\mathbf{4}, \mathbf{1}, \mathbf{2})$	$\bar{H}^c U_R^\top U_c^\top$	0	0	0	
S	$(\mathbf{1}, \mathbf{1}, \mathbf{1})$	S	1	0	0	
G	$(\mathbf{6}, \mathbf{1}, \mathbf{1})$	$U_c G U_c^\top$	1	0	0	
h	$(\mathbf{1}, \mathbf{2}, \mathbf{2})$	$U_L h U_R^\top$	0	1	0	
N	$(\mathbf{1}, \mathbf{1}, \mathbf{1})$	N	$1/2$	-1	0	
\bar{N}	$(\mathbf{1}, \mathbf{1}, \mathbf{1})$	\bar{N}	0	1	0	
EXTRA HIGGS SUPERFIELDS						
h'	$(\mathbf{15}, \mathbf{2}, \mathbf{2})$	$U_c^* U_L h' U_R^\top U_c^\top$	0	1	0	
\bar{h}'	$(\mathbf{15}, \mathbf{2}, \mathbf{2})$	$U_c U_L \bar{h}' U_R^\top U_c^\dagger$	1	-1	0	
ϕ	$(\mathbf{15}, \mathbf{1}, \mathbf{3})$	$U_c U_R \phi U_R^\dagger U_c^\dagger$	0	0	0	
$\bar{\phi}$	$(\mathbf{15}, \mathbf{1}, \mathbf{3})$	$U_c U_R \bar{\phi} U_R^\dagger U_c^\dagger$	1	0	0	

TABLE 1: The representations and transformations under G_{PS} as well as the extra global charges of the superfields of our model ($U_c \in SU(4)_c$, $U_L \in SU(2)_L$, $U_R \in SU(2)_R$ and \top, \dagger and $*$ stand for the transpose, the hermitian conjugate and the complex conjugate of a matrix respectively).

since, after the breaking of G_{PS} to G_{SM} , the third family fermion masses originate from a unique term of the underlying GUT as follows:

$$y_{33} F_3 \langle h \rangle F_3^c = y_{33} (-v_2 t t^c + v_1 b b^c + v_1 \tau \tau^c) + \dots, \text{ where } v_i = \langle H_i \rangle. \quad (6)$$

A moderate violation of YU can be accommodated by adding two new Higgs superfields h' and \bar{h}' with

$$h' = \begin{pmatrix} h'_2 & h'_1 \end{pmatrix} \text{ and } \bar{h}' = \begin{pmatrix} \bar{h}'_2 & \bar{h}'_1 \end{pmatrix}. \quad (7)$$

In accordance with the global symmetries imposed (see Table 1), h' can couple to FF^c since $FF^c = (\mathbf{15}, \mathbf{2}, \mathbf{2})$, whereas \bar{h}' can give mass to the color non-singlet components of h' through a superpotential term $m\bar{h}'h'$ ($m \sim M_{\text{GUT}} \simeq 2 \times 10^{16}$ GeV), which corresponds to the following G_{PS} invariant quantity:

$$m \text{Tr} \left(\bar{h}' \epsilon h'^\top \epsilon \right), \text{ where } \epsilon = \begin{pmatrix} 0 & 1 \\ -1 & 0 \end{pmatrix} \quad (8)$$

and Tr denotes trace taken w.r.t. the $SU(4)_c$ and $SU(2)_L$ indices. Other important superpotential terms, which, being non-renormalizable, are suppressed by the string scale $M_S \simeq 5 \times 10^{17}$ GeV, are

$$\bar{H}^c H^c \bar{h}' h = (\mathbf{1}, \mathbf{1}, \mathbf{1} \times \mathbf{1} + \mathbf{3} \times \mathbf{3}), \quad (9)$$

since

$$\begin{aligned} \bar{H}^c H^c &= (\mathbf{4}, \mathbf{1}, \mathbf{2})(\bar{\mathbf{4}}, \mathbf{1}, \mathbf{2}) = (\mathbf{15}, \mathbf{1}, \mathbf{1} + \mathbf{3}) + \dots, \\ \bar{h}' h &= (\mathbf{15}, \mathbf{2}, \mathbf{2})(\mathbf{1}, \mathbf{2}, \mathbf{2}) = (\mathbf{15}, \mathbf{1}, \mathbf{1} + \mathbf{3}) + \dots. \end{aligned}$$

We see that, in Eq. (9), there are two independent couplings: a coupling between the $SU(2)_R$ singlets in $\bar{H}^c H^c$ and $\bar{h}' h$, $(\bar{H}^c H^c)_1 \bar{h}' h$, and a coupling between their triplets, $(\bar{H}^c H^c)_3 \bar{h}' h$. As it turns out, the singlet coupling provides us with an adequate deviation from YU for $\mu < 0$. On the other hand, $\mu > 0$ requires a stronger deviation.

2.2 The $\mu > 0$ Case

The necessary deviation from YU for $\mu > 0$ can be obtained by a further enlargement of the Higgs sector so that contributions to the coupling between h and \bar{h}' from renormalizable terms are also allowed. To this end, we introduce two additional Higgs superfields ϕ , $\bar{\phi}$. The superfield $\bar{\phi}$ is aimed to give superheavy masses to the color non-singlets in ϕ through a term $\bar{\phi}\phi$, whose coefficient is of order M_{GUT} . The superfield ϕ , on the other hand, yields the unsuppressed coupling $\lambda_3 \phi \bar{h}' h$ (with λ_3 being a dimensionless constant), which overshadows the coupling $(\bar{H}^c H^c)_3 \bar{h}' h$ and corresponds to the G_{PS} invariant term

$$\lambda_3 \text{Tr} \left(\bar{h}' \epsilon \phi h^T \epsilon \right). \quad (10)$$

During the spontaneous breaking of G_{PS} to G_{SM} , ϕ acquires VEV in the SM singlet direction. Therefore,

$$\langle \phi \rangle = v_\phi \left(T^{15}, 1, \frac{\sigma_3}{\sqrt{2}} \right), \quad (11)$$

where $v_\phi \sim M_{\text{GUT}}$ and the structure of $\langle \phi \rangle$ w.r.t. G_{PS} is shown with

$$T^{15} = \frac{1}{2\sqrt{3}} \text{diag} \left(1, 1, 1, -3 \right) \quad \text{and} \quad \sigma_3 = \text{diag} \left(1, -1 \right). \quad (12)$$

Expanding the superfields in Eq. (7) as linear combination of the fifteen generators T^a of $SU(4)_c$ with the normalization $\text{Tr}(T^a T^b) = \delta^{ab}$ and denoting the SM

singlet components with the superfield symbol, we can easily establish the following identities:

$$\text{Tr} \left(\bar{h}' \epsilon h'^T \epsilon \right) = \bar{h}'^T \epsilon h'_2 + h'^T \epsilon \bar{h}'_2 + \dots, \quad (13)$$

$$\text{Tr} \left(\bar{h}' \epsilon (T^{15}, 1, \sigma_3) h^T \epsilon \right) = \left(\bar{h}'^T \epsilon h_2 - h'^T \epsilon \bar{h}'_2 \right), \quad (14)$$

where the notation of Eq. (11) has been applied.

Inserting Eq. (11) in Eq. (10), employing Eqs. (13) and (14), and collecting Eqs. (8) and (10) together, we get the mass terms

$$m \bar{h}'^T \epsilon (h'_2 + \alpha_2 h_2) + m \left(h'^T + \alpha_1 h^T \right) \epsilon \bar{h}'_2, \quad (15)$$

where the mixing effects are included in the following coefficients:

$$\alpha_1 = -\alpha_2 = -\lambda_3 v_\phi / \sqrt{2}m. \quad (16)$$

2.3 The $\mu < 0$ Case

In the $\mu < 0$ case, an adequate violation of YU can be achieved (without the inclusion of ϕ and $\bar{\phi}$) predominantly via the non-renormalizable $SU(2)_R$ singlet coupling $\lambda_1 (\bar{H}^c \bar{H}^c)_{\mathbf{1}} h^c h / M_S$ (with λ_1 being a dimensionless constant), which corresponds to the G_{PS} invariant term

$$\frac{\lambda_1}{M_S} \text{Tr} \left(\bar{h}' \epsilon (\bar{H}^{cT} H^{cT})_{\mathbf{1}} h^T \epsilon \right). \quad (17)$$

During the spontaneous breaking of G_{PS} to G_{SM} , H^c and \bar{H}^c acquire VEVs in the SM singlet direction. Therefore,

$$\left(\langle \bar{H}^{cT} \rangle \langle H^{cT} \rangle \right)_{\mathbf{1}} = v_{H^c}^2 \left(T_{H^c}, 1, \frac{\sigma_0}{2} \right), \quad (18)$$

where $v_{H^c} \sim M_{\text{GUT}}$ and the notation of Eq. (11) has been applied with

$$T_{H^c} = \text{diag} \left(0, 0, 0, 1 \right) \quad \text{and} \quad \sigma_0 = \text{diag} \left(1, 1 \right). \quad (19)$$

Expanding the superfields in Eq. (7) as we did in deriving Eq. (14), we obtain the following identity:

$$\text{Tr} \left(\bar{h}' \epsilon (T_{H^c}, 1, \sigma_0) h^T \epsilon \right) = -\sqrt{3} \left(\bar{h}'^T \epsilon h_2 + h'^T \epsilon \bar{h}'_2 \right) / 2. \quad (20)$$

Inserting Eq. (18) in Eq. (17), employing Eqs. (13) and (20), and collecting Eqs. (8) and (17) together, we end up again with Eq. (15) but with

$$\alpha_1 = \alpha_2 = -\frac{\sqrt{3} \lambda_1}{4 M_S m} v_{H^c}^2, \quad (21)$$

which are suppressed by M_{GUT}/M_S .

2.4 Yukawa Quasi-Unification Conditions

It is obvious from Eq. (15) that we obtain two combinations of superheavy massive fields

$$\bar{h}'_1, H'_1 \text{ and } \bar{h}'_2, H'_2, \text{ where } H'_i = \frac{h'_i + \alpha_i h_i}{\sqrt{1 + |\alpha_i|^2}}, i = 1, 2. \quad (22)$$

The electroweak doublets H_i , which remain massless at the GUT scale, are orthogonal to the H'_i directions:

$$H_i = \frac{-\alpha_i^* h'_i + h_i}{\sqrt{1 + |\alpha_i|^2}}. \quad (23)$$

Solving Eqs. (22) and (23) w.r.t. h_i and h'_i , we obtain

$$h_i = \frac{H_i + \alpha_i^* H'_i}{\sqrt{1 + |\alpha_i|^2}} \text{ and } h'_i = \frac{-\alpha_i H_i + H'_i}{\sqrt{1 + |\alpha_i|^2}}. \quad (24)$$

Consequently, the third family fermion masses are now generated by the following terms (compare with Eq. (6)):

$$y_{33} F_3 \langle h \rangle F_3^c + 2y'_{33} F_3 \langle h' \rangle F_3^c = \\ y_{33} \left(-\frac{1 - \rho \alpha_2 / \sqrt{3}}{\sqrt{1 + |\alpha_2|^2}} v_2 t t^c + \frac{1 - \rho \alpha_1 / \sqrt{3}}{\sqrt{1 + |\alpha_1|^2}} v_1 b b^c + \frac{1 + \sqrt{3} \rho \alpha_1}{\sqrt{1 + |\alpha_1|^2}} v_1 \tau \tau^c \right) + \dots$$

where $\rho = y'_{33}/y_{33}$ with $0 < \rho < 1$ and the color non-singlet components of h'_i are included in the ellipsis. The fields H'_i , being superheavy, contribute neither to the running of renormalization group equations (RGEs) nor to the masses of the fermions. Consequently, the asymptotic exact YU in Eq. (5) can be replaced by a set of asymptotic Yukawa quasi-unification conditions (YQUCs):

$$h_t : h_b : h_\tau = \left| \frac{1 - \rho \alpha_2 / \sqrt{3}}{\sqrt{1 + |\alpha_2|^2}} \right| : \left| \frac{1 - \rho \alpha_1 / \sqrt{3}}{\sqrt{1 + |\alpha_1|^2}} \right| : \left| \frac{1 + \sqrt{3} \rho \alpha_1}{\sqrt{1 + |\alpha_1|^2}} \right|. \quad (25)$$

Substituting Eqs. (16) and (21) into Eq. (25), we obtain

$$h_t : h_b : h_\tau = \begin{cases} (1 + c) : (1 - c) : (1 + 3c) & \text{with } 0 < c < 1 \quad \text{for } \mu > 0 \\ (1 - c) : (1 - c) : (1 + 3c) & \text{with } -1/3 < c < 0 \quad \text{for } \mu < 0 \end{cases}. \quad (26)$$

For simplicity, we restricted ourselves to real values of c only, where $c = \rho \alpha_1 / \sqrt{3}$.

The deviation from YU can be estimated by defining the following relative splittings:

$$\delta h_{b[\tau]} = \frac{h_{b[\tau]} - h_t}{h_t} = \begin{cases} -2c/(1 + c) [2c/(1 + c)] & \text{for } \mu > 0 \\ 0 [4c/(1 + c)] & \text{for } \mu < 0 \end{cases}. \quad (27)$$

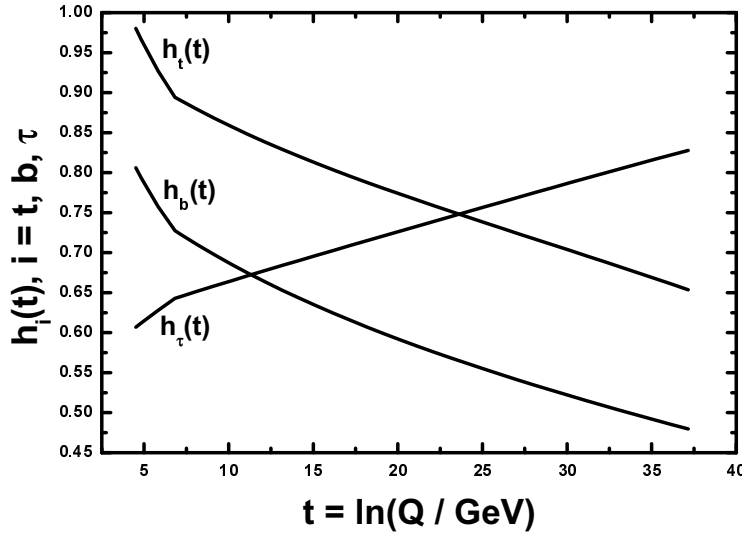


FIGURE 1: A running of the Yukawa coupling constants from $Q = M_{\text{GUT}}$ to $Q = M_Z$ for $m_b(M_Z) = 2.888 \text{ GeV}$, $\mu > 0$, $m_{\text{LSP}} = 200 \text{ GeV}$ and $\Delta_{\tilde{\tau}_2} = 1$ corresponding to $\tan \beta \simeq 58$.

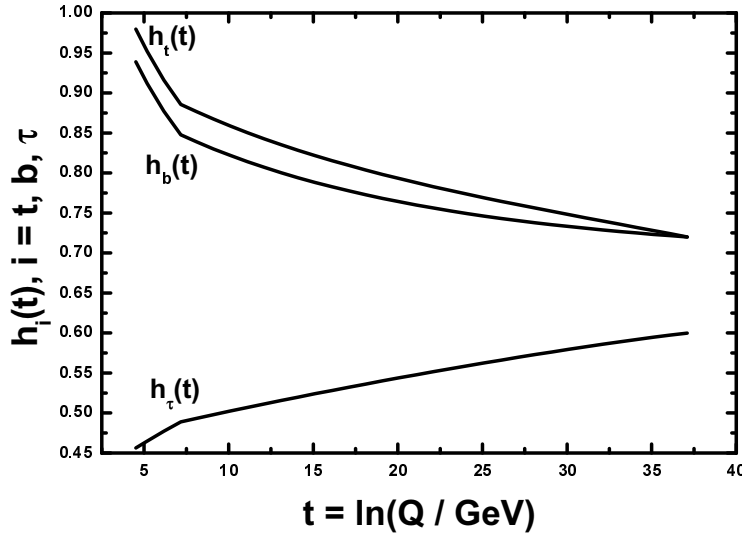


FIGURE 2: A running of the Yukawa coupling constants from $Q = M_{\text{GUT}}$ to $Q = M_Z$ for $m_b(M_Z) = 2.888 \text{ GeV}$, $\mu < 0$, $m_{\text{LSP}} = 350 \text{ GeV}$ and $\Delta_{\tilde{\tau}_2} = 0$ corresponding to $\tan \beta \simeq 47$.

3 The resulting CMSSM

Below M_{GUT} , the particle content of our models reduces to this of MSSM (modulo SM singlets). We assume universal soft SUSY breaking scalar masses m_0 , gaugino masses $M_{1/2}$ and trilinear scalar couplings A_0 at M_{GUT} . Therefore, the resulting MSSM is the so-called CMSSM [1] supplemented by a suitable YQUC from the set in Eq. (26). Let us emphasize that the specific relations between α_1 and α_2 given in Eq. (16) [Eq. (21)] for $\mu > 0$ [$\mu < 0$] ensure a SUSY spectrum which leads to successful radiative electroweak symmetry breaking (REWSB) and a neutral LSP in a large fraction of the parametric space in the framework of the CMSSM (and not in a general version of MSSM).

We integrate the two-loop RGEs for the gauge and Yukawa coupling constants and the one-loop ones for the soft SUSY breaking terms between M_{GUT} and a common SUSY threshold $M_{\text{SUSY}} \simeq (m_{\tilde{t}_1} m_{\tilde{t}_2})^{1/2}$ ($\tilde{t}_{1,2}$ are the stop mass eigenstates) determined in consistency with the SUSY spectrum. At M_{SUSY} , we impose REWSB, evaluate the SUSY spectrum and incorporate the SUSY corrections to the b and τ mass [6, 7, 12]. The corrections to m_τ (almost 4%) lead [32] to a small decrease [increase] of $\tan \beta$ for $\mu > 0$ [$\mu < 0$]. From M_{SUSY} to M_Z , the running of gauge and Yukawa coupling constants is continued using the SM RGEs.

For presentation purposes, $M_{1/2}$ and m_0 can be replaced [32] by the LSP mass, m_{LSP} , and the relative mass splitting, $\Delta_{\tilde{\tau}_2}$, between the LSP and the lightest stau $\tilde{\tau}_2$. For simplicity, we restrict this presentation to the $A_0 = 0$ case (for $A_0 \neq 0$, see Refs. [9, 33]). So, our free input parameters are

$$\text{sign}(\mu), \ m_{\text{LSP}}, \ \Delta_{\tilde{\tau}_2}, \ \text{with} \ \Delta_{\tilde{\tau}_2} = (m_{\tilde{\tau}_2} - m_{\text{LSP}})/m_{\text{LSP}}.$$

For any given $m_b(M_Z)$ in the range in Eq. (1) with fixed masses for the top quark $m_t(m_t) = 166$ GeV and the tau lepton $m_\tau(M_Z) = 1.746$ GeV, we can determine the parameters c and $\tan \beta$ at M_{SUSY} so that the corresponding YQUC in Eq. (26) is satisfied. Consequently, for any given $m_b(M_Z)$, a prediction for $\tan \beta$ can be made, in contrast to the original version of CMSSM [1].

In Fig. 1 [Fig. 2], we present a Yukawa coupling constant running from M_{GUT} to M_Z for the central value of $m_b(M_Z) = 2.888$ GeV. At M_{GUT} , we apply Eq. (26) with $c = 0.154$ [$c = -0.043$] (corresponding to $\tan \beta \simeq 58$ [$\tan \beta \simeq 47$] at M_{SUSY}) for $\mu > 0$ [$\mu < 0$], $m_{\text{LSP}} = 200$ GeV [$m_{\text{LSP}} = 350$ GeV] and $\Delta_{\tilde{\tau}_2} = 1$ [$\Delta_{\tilde{\tau}_2} = 0$]. The kinks on the various curves correspond to the point where the MSSM RGEs are replaced by the SM ones. We observe that, for $\mu > 0$, h_τ and h_b split from h_t by the same amount but in opposite directions with h_b becoming smaller than h_t (see Fig. 1), while, for $\mu < 0$, h_t and h_b remain unified (see Fig. 2).

In Fig. 3 [Fig. 4], we present the values of the mass parameters m_A , m_0 , $M_{1/2}$ and M_{SUSY} versus m_{LSP} for $\mu > 0$ [$\mu < 0$], $\Delta_{\tilde{\tau}_2} = 1$ [$\Delta_{\tilde{\tau}_2} = 0$] (see Sec. 5.1 [Sec. 5.2]) and with $m_b(M_Z) = 2.888$ GeV. We observe that $m_0 \gg M_{1/2}$ [$m_0 \ll M_{1/2}$] and $m_A \lesssim 2m_{\text{LSP}}$ [$m_A \ll 2m_{\text{LSP}}$] for $\mu > 0$ [$\mu < 0$]. The relation between m_{LSP} and m_A or $m_{\tilde{\tau}_2}$ is crucial for the reduction of the LSP relic abundance (see Sec. 4.1).

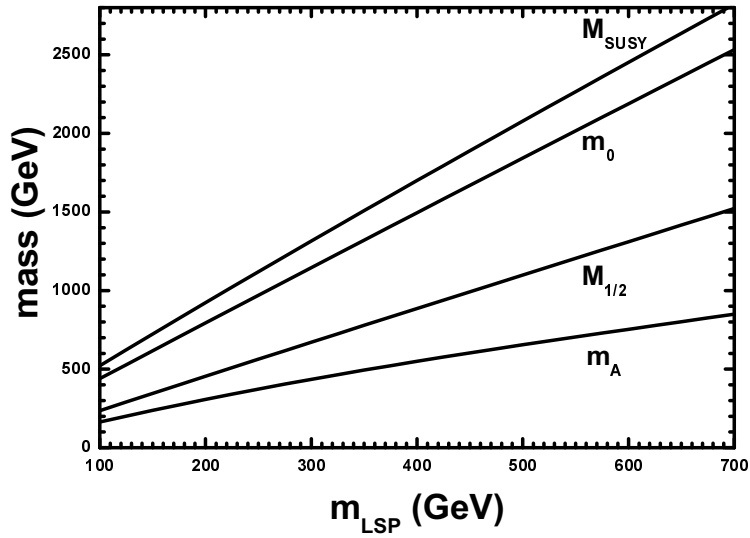


FIGURE 3: The mass parameters m_A , m_0 , $M_{1/2}$ and M_{SUSY} versus m_{LSP} for $\mu > 0$, $m_b(M_Z) = 2.888$ GeV and $\Delta_{\tilde{\tau}_2} = 1$.

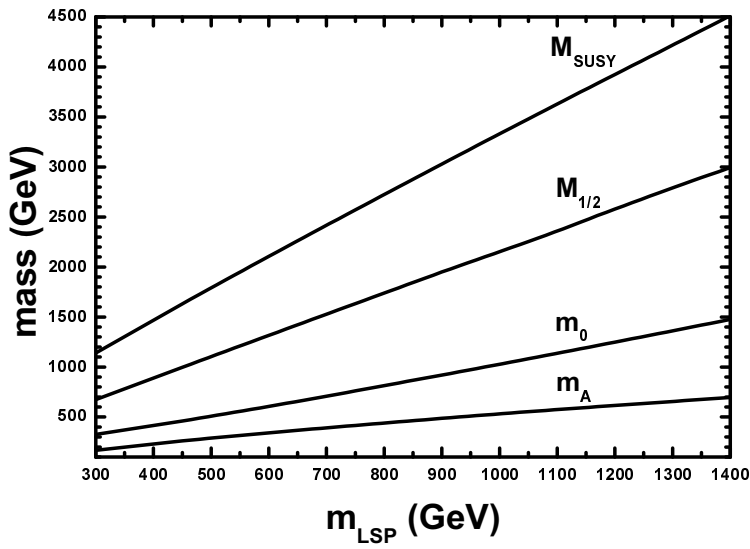


FIGURE 4: The mass parameters m_A , m_0 , $M_{1/2}$ and M_{SUSY} versus m_{LSP} for $\mu < 0$, $m_b(M_Z) = 2.888$ GeV and $\Delta_{\tilde{\tau}_2} = 0$.

4 Cosmological and Phenomenological Constraints

The parameter space of our models can be restricted by using a number of phenomenological and cosmological constraints. We will now briefly discuss these requirements (for similar recent analyses, see Refs. [14, 15, 16, 34]).

4.1 Cold Dark Matter Considerations

According to the WMAP results [18], the 95% c.l. range for the CDM abundance is

$$\Omega_{\text{CDM}} h^2 = 0.1126_{-0.0181}^{+0.0161}. \quad (28)$$

In the context of the CMSSM, the LSP can be the lightest neutralino $\tilde{\chi}$. It naturally arises [35] as a CDM candidate. We require its relic abundance, $\Omega_{\text{LSP}} h^2$, not to exceed the upper bound derived from Eq. (28) (the lower bound is not considered since other production mechanisms of LSPs may be present too [36, 37] and/or other CDM candidates [38, 39] may also contribute to $\Omega_{\text{CDM}} h^2$):

$$\Omega_{\text{LSP}} h^2 \lesssim 0.13. \quad (29)$$

For each sign of μ , an upper bound on m_{LSP} (or $m_{\tilde{\chi}}$) can be derived from Eq. (29). We calculate $\Omega_{\text{LSP}} h^2$ using the publicly available code `micrOMEGAs` [40] (not the latest version [41]). This includes accurately thermally averaged exact tree-level cross sections of all possible (co)annihilation processes, treats poles properly and uses one-loop QCD (not SUSY QCD [41, 43]) corrections to the Higgs decay widths and couplings to fermions [42]. Good agreement between this code and other independent calculations of $\Omega_{\text{LSP}} h^2$ which include the A -pole effect and neutralino-stau coannihilation is recently reported in the first paper of Ref. [9] and in Ref. [43].

In most of the parameter space of the CMSSM, the LSP is an almost pure bino and $\Omega_{\text{LSP}} h^2$ increases with m_{LSP} . Therefore, Eq. (29) sets a very stringent upper limit on the LSP mass [44]. However, as pointed out in Refs. [45, 46], a substantial reduction of $\Omega_{\text{LSP}} h^2$ can be achieved in some regions of the parameter space thanks to two mechanisms: the A -pole effect and the bino-slepton coannihilations. The first is activated for $\tan \beta > 40$ [$\tan \beta \simeq 30 - 35$] for $\mu > 0$ [$\mu < 0$], where the presence of a resonance ($2m_{\text{LSP}} \simeq m_A$) in the LSP annihilation via a s -channel exchange of an A -boson is possible. On the other hand, coannihilations can be activated for every $\tan \beta$ and both signs of μ , but this requires a proximity between the masses of the LSP and the next-to-LSP, which turns out to be the $\tilde{\tau}_2$ for $\tan \beta > 10$ [46] and not too large values of A_0 [47] or m_0 [48]. For fixed m_{LSP} , $\Omega_{\text{LSP}} h^2$ decreases with $\Delta_{\tilde{\tau}_2}$, since the $\tilde{\chi} - \tilde{\tau}_2$ coannihilations become more efficient. So the CDM criterion can be used for restricting $\Delta_{\tilde{\tau}_2}$.

Our models give us the opportunity to discuss how both these reduction mechanisms operate. As we noticed from Figs. 3 and 4, for $\mu > 0$, there is a significant region dominated by the A -pole effect, while, for $\mu < 0$, the $\tilde{\chi} - \tilde{\tau}_2$ coannihilation is the only available reduction mechanism.

4.2 Branching Ratio of $b \rightarrow s\gamma$

Taking into account the recent experimental results [20] on $\text{BR}(b \rightarrow s\gamma)$ and combining [9] appropriately the various experimental and theoretical errors involved, we obtain the following 95% c.l. range:

$$\text{a)} 1.9 \times 10^{-4} \lesssim \text{BR}(b \rightarrow s\gamma) \quad \text{and} \quad \text{b)} \text{BR}(b \rightarrow s\gamma) \lesssim 4.6 \times 10^{-4}. \quad (30)$$

We compute $\text{BR}(b \rightarrow s\gamma)$ by using an updated version of the relevant calculation contained in the `micrOMEGAs` package [40]. In this code, the SM contribution is calculated using the formalism of Ref. [49]. The charged Higgs boson, H^\pm , contribution is evaluated by including the next-to-leading order (NLO) QCD corrections from Ref. [50] and the $\tan\beta$ enhanced contributions from Ref. [51]. The dominant SUSY contribution, $\text{BR}(b \rightarrow s\gamma)|_{\text{SUSY}}$, includes resummed NLO SUSY QCD corrections from Ref. [51], which hold for large $\tan\beta$. The H^\pm contribution interferes constructively with the SM contribution, whereas $\text{BR}(b \rightarrow s\gamma)|_{\text{SUSY}}$ interferes destructively [constructively] with the other two contributions for $\mu > 0$ [$\mu < 0$]. Although the improvements of Ref. [52] are not included in this routine, their impact is not important for $\mu > 0$, whereas, for $\mu < 0$, they are not expected to change essentially our conclusions. The SM plus H^\pm contribution and the $\text{BR}(b \rightarrow s\gamma)|_{\text{SUSY}}$ decrease as m_{LSP} increases and so a lower bound on m_{LSP} can be derived from Eq. (30a) [Eq. (30b)] for $\mu > 0$ [$\mu < 0$] with the bound for $\mu < 0$ being much more restrictive.

4.3 Muon Anomalous Magnetic Moment

The deviation, δa_μ , of the measured value of the muon anomalous magnetic moment, a_μ , from its predicted value in the SM, a_μ^{SM} , can be attributed to SUSY contributions arising from chargino-sneutrino and neutralino-smuon loops. The quantity δa_μ is calculated by using the `micrOMEGAs` routine based on the formulas of Ref. [53]. The absolute value of the result decreases as m_{LSP} increases and its sign is positive [negative] for $\mu > 0$ [$\mu < 0$].

On the other hand, the calculation of a_μ^{SM} is not yet stabilized mainly because of the instability of the hadronic vacuum polarization contribution. According to the most up-to-date evaluation of this contribution in Ref. [54], there is still a discrepancy between the findings based on the e^+e^- annihilation data and the ones based on the τ -decay data. Taking into account these results and the recently announced experimental measurements [21] on a_μ , we impose the following 95% c.l. ranges:

$$\text{a)} -0.53 \times 10^{-10} \lesssim \delta a_\mu \quad \text{and} \quad \text{b)} \delta a_\mu \lesssim 44.7 \times 10^{-10}, \quad e^+e^- \text{-based}; \quad (31)$$

$$\text{a)} -13.5 \times 10^{-10} \lesssim \delta a_\mu \quad \text{and} \quad \text{b)} \delta a_\mu \lesssim 28.4 \times 10^{-10}, \quad \tau \text{-based}. \quad (32)$$

A lower bound on m_{LSP} can be derived from Eq. (31b) [Eq. (32a)] for $\mu > 0$ [$\mu < 0$]. Although the $\mu < 0$ case can not be excluded [55], it is considered as quite disfavored [56] because of the poor τ -decay data.

4.4 Collider Bounds

For our analysis, the only relevant collider bound is the 95% c.l. LEP bound [22] on the lightest CP-even neutral Higgs boson, h , mass

$$m_h \gtrsim 114.4 \text{ GeV}, \quad (33)$$

which gives a [almost always the absolute] lower bound on m_{LSP} for $\mu < 0$ [$\mu > 0$]. The SUSY contributions to m_h are calculated at two loops by employing the program **FeynHiggsFast** [57] contained in the **micrOMEGAs** package [40].

5 Restrictions on the SUSY Parameters

Applying the cosmological and phenomenological requirements given in Sec. 4, we delineate on the $m_{\text{LSP}} - \Delta_{\tilde{\tau}_2}$ plane the allowed parameter space of our models in Secs. 5.1 and 5.2 for $\mu > 0$ and $\mu < 0$ respectively. For simplicity, $\alpha_s(M_Z)$ is fixed to its central experimental value (equal to 0.1185) throughout our calculation. Note that allowing it to vary in its 95% c.l. experimental range, 0.1145 – 0.1225, the range of $m_b(M_Z)$ in Eq. (1) would be slightly widened. This would lead to a sizeable enlargement of the allowed area for $\mu > 0$ due to the sensitivity of $\Omega_{\text{LSP}} h^2$ to the b -quark mass (see Sec. 5.1). On the contrary, our results for $\mu < 0$ would be essentially unaffected, since the LSP annihilation to $b\bar{b}$ via an A -boson exchange gives a subdominant contribution to $\Omega_{\text{LSP}} h^2$ (see Sec. 5.2).

5.1 The $\mu > 0$ Case

The restrictions on the $m_{\text{LSP}} - \Delta_{\tilde{\tau}_2}$ plane with $m_b(M_Z) = 2.888$ GeV are shown in Fig. 5 as solid lines, while the upper bound on m_{LSP} from Eq. (29) for $m_b(M_Z) = 2.684$ GeV [$m_b(M_Z) = 3.092$ GeV] is depicted by a dashed [dotted] line. Needless to say that the constraints from Eqs. (30b) and (32a) do not restrict the parameters, since they are always satisfied for $\mu > 0$.

We observe the following:

- The lower bounds on m_{LSP} are not so sensitive to the variations of $m_b(M_Z)$.
- The lower bound on m_{LSP} from Eq. (33) overshadows all others.
- The LSP annihilation via the s -channel exchange of an A -boson is by far the dominant (co)annihilation process near the almost vertical part of the line corresponding to the upper bound on m_{LSP} from Eq. (29). This can be explained by considering Fig. 6, where we draw m_A and M_{SUSY} versus m_{LSP} for various $\Delta_{\tilde{\tau}_2}$'s and the central value of $m_b(M_Z)$. We see that m_A is always smaller than $2m_{\text{LSP}}$ but close to it. We also observe that, as m_{LSP} or $\Delta_{\tilde{\tau}_2}$ increases, we move away from the A -pole which, thus, becomes less efficient. As a consequence, $\Omega_{\text{LSP}} h^2$ increases with m_{LSP} or $\Delta_{\tilde{\tau}_2}$.

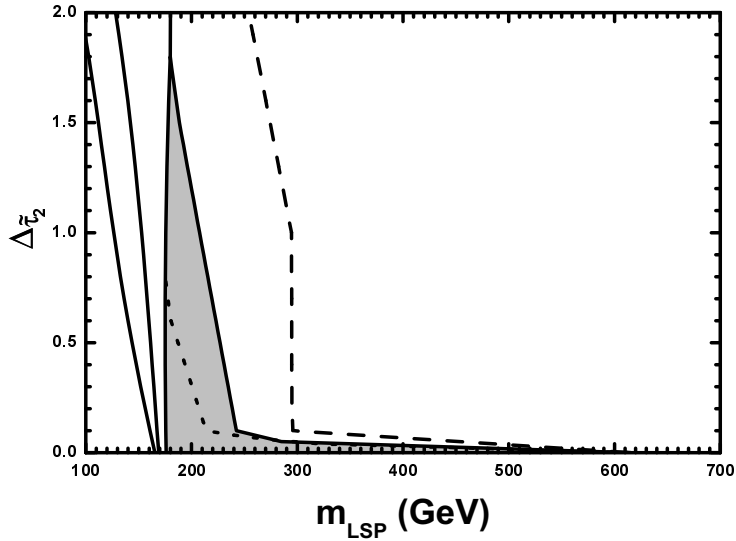


FIGURE 5: *Restrictions on the $m_{\text{LSP}} - \Delta_{\tilde{\tau}_2}$ plane for $\mu > 0$. From left to right, the solid lines depict the lower bounds on m_{LSP} from Eq. (31b), (30a), (33) and the upper bound on m_{LSP} from Eq. (29) for $m_b(M_Z) = 2.888$ GeV. The dashed [dotted] line depicts the bound on m_{LSP} from Eq. (29) for $m_b(M_Z) = 2.684$ GeV [3.092 GeV]. The allowed area for $m_b(M_Z) = 2.888$ GeV is shaded.*

- The upper bound on m_{LSP} from Eq. (29) is extremely sensitive to the variations of $m_b(M_Z)$. Especially sensitive is the almost vertical part of the line corresponding to this bound, where, as we saw above, the LSP annihilation via an A -boson exchange in the s -channel is by far the dominant process. This extreme sensitivity can be understood from Fig. 7, where m_A is depicted versus m_{LSP} for the lower, upper and central values of $m_b(M_Z)$ in Eq. (1). We see that, as $m_b(M_Z)$ decreases, m_A increases and approaches $2m_{\text{LSP}}$. The A -pole annihilation is then enhanced and $\Omega_{\text{LSP}} h^2$ is drastically reduced causing an increase of the upper bound on m_{LSP} .
- For $\Delta_{\tilde{\tau}_2} < 0.25$, bino-stau coannihilations [46] take over leading to a very pronounced reduction of $\Omega_{\text{LSP}} h^2$, thereby increasing the upper limit on m_{LSP} .

For $m_b(M_Z) = 2.888$ GeV, the allowed ranges of m_{LSP} and $\Delta_{\tilde{\tau}_2}$ are

$$176 \text{ GeV} \lesssim m_{\text{LSP}} \lesssim 615 \text{ GeV} \text{ and } 0 \lesssim \Delta_{\tilde{\tau}_2} \lesssim 1.8. \quad (34)$$

5.2 The $\mu < 0$ Case

As is seen from Fig. 4, $2m_{\text{LSP}} \gg m_A$ in the $\mu < 0$ case. So, the LSP annihilation to $b\bar{b}$ via the s -channel exchange of an A -boson is not enhanced as for $\mu > 0$ (the

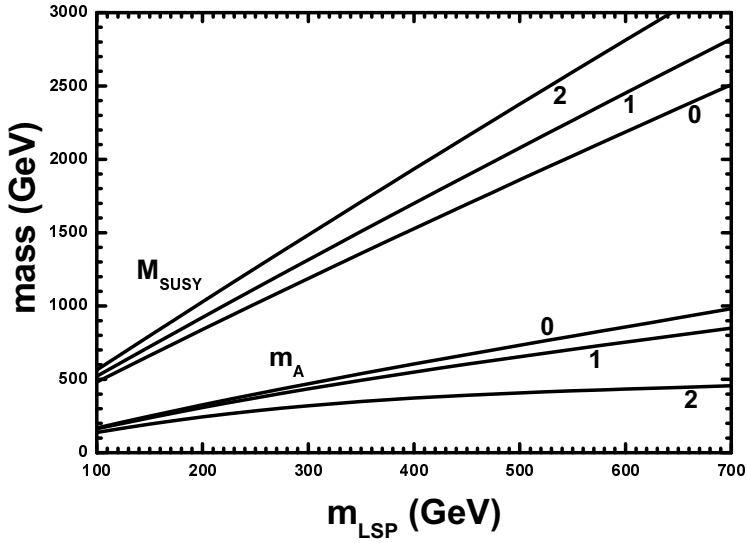


FIGURE 6: The mass parameters m_A and M_{SUSY} versus m_{LSP} for $\mu > 0$, $m_b(M_Z) = 2.888$ GeV and various values of $\Delta\tilde{\tau}_2$, which are indicated on the curves.

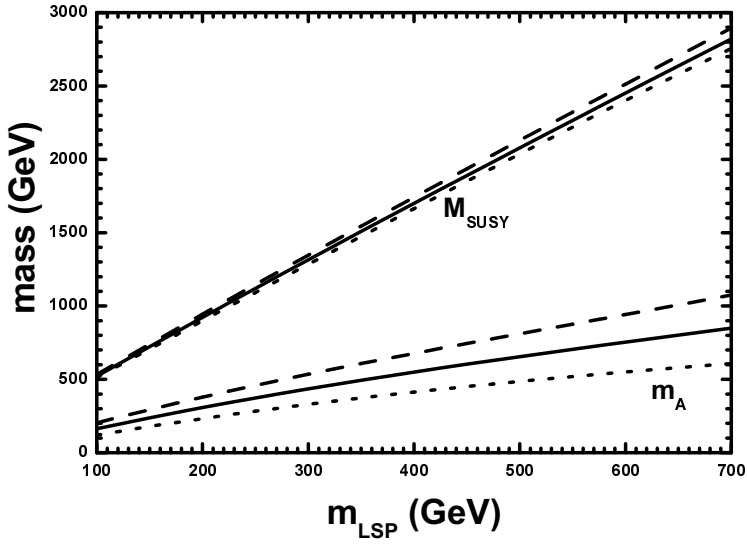


FIGURE 7: The mass parameters m_A and M_{SUSY} versus m_{LSP} for $\mu > 0$, $\Delta\tilde{\tau}_2 = 1$ and with $m_b(M_Z) = 2.684$ GeV (dashed lines), 3.092 GeV (dotted lines) or 2.888 GeV (solid lines).

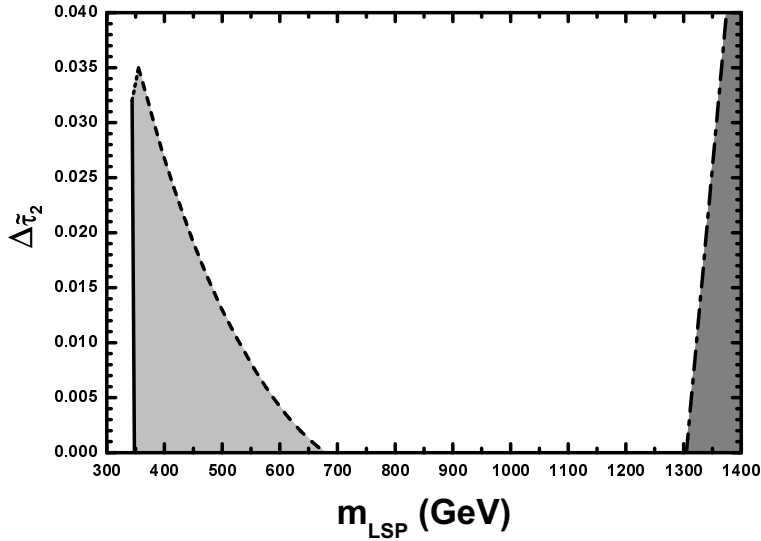


FIGURE 8: *Restrictions on the $m_{\text{LSP}} - \Delta_{\tilde{\tau}_2}$ plane for $\mu < 0$ and $m_b(M_Z)$ in the range of Eq. (1). The solid [dot-dashed] line corresponds to the lower bound on m_{LSP} from Eq. (32a) [Eq. (30b)]. The dashed [dotted] line corresponds to the upper bound on $m_{\text{LSP}} [\Delta_{\tilde{\tau}_2}]$ from Eq. (29).*

important annihilation channels, for $\mu < 0$, are not only the ones with fermions $f\bar{f}$ in the final state, but also with HZ , $W^\pm H^\mp$ and hA [43, 58]). As a consequence, the only available mechanism for reducing the $\Omega_{\text{LSP}} h^2$ is the $\tilde{\chi} - \tilde{\tau}_2$ coannihilation [46] (for an updated study, see also Ref. [59]), which becomes efficient when $\Delta_{\tilde{\tau}_2} < 0.25$.

The restrictions from all the requirements imposed on the $m_{\text{LSP}} - \Delta_{\tilde{\tau}_2}$ plane for any $m_b(M_Z)$ in Eq. (1) are presented in Fig. 8. The lower bound on m_{LSP} from Eq. (32a) corresponds to $m_b(M_Z) \simeq 3.092$ GeV and is represented by a solid line. The maximal $\Delta_{\tilde{\tau}_2} (\simeq 0.032)$ on this line yields $\Omega_{\text{LSP}} h^2 \simeq 0.13$ for the same value of $m_b(M_Z)$. As $m_b(M_Z)$ decreases, the maximal $\Delta_{\tilde{\tau}_2}$ from Eq. (29) increases along the dotted line and reaches its overall maximal value at $\Delta_{\tilde{\tau}_2} \simeq 0.035$ for $m_b(M_Z) \simeq 2.684$ GeV. The upper bound on m_{LSP} from Eq. (29) is achieved for $m_b(M_Z) \simeq 2.684$ GeV and corresponds to the dashed line. In the lightly shaded region allowed by Eqs. (32a) and (29), we find

$$348 \text{ GeV} \lesssim m_{\text{LSP}} \lesssim 680 \text{ GeV} \text{ and } 0 \lesssim \Delta_{\tilde{\tau}_2} \lesssim 0.035. \quad (35)$$

The maximal m_{LSP} is achieved at $\Delta_{\tilde{\tau}_2} = 0$ yielding $\text{BR}(b \rightarrow s\gamma) \simeq 5.8 \times 10^{-4}$.

On the other hand, the lower bound on m_{LSP} (dot-dashed line) from Eq. (30b) corresponds to $m_b(M_Z) \simeq 3.092$ GeV. In the corresponding allowed (dark shaded) area in Fig. 8,

$$m_{\text{LSP}} \gtrsim 1305.04 \text{ GeV} \quad (36)$$

with the minimal m_{LSP} achieved at $\Delta_{\tilde{\tau}_2} = 0$ and yielding $\Omega_{\text{LSP}} h^2 \simeq 0.65$. Note that the NLO corrections to $\text{BR}(b \rightarrow s\gamma)$ (see Sec. 4.2) drastically reduce this lower bound on m_{LSP} . It is worth mentioning that, in the second paper of Ref. [32] (which adopts the opposite sign convention for μ), where the $\tan \beta$ enhanced and NLO SUSY QCD corrections were not included, the reduction was considerably higher and yielded a much less stringent restriction.

Combining Eqs. (35) and (36), it is obvious that we are left with no simultaneously allowed region. Needless to say that the constraints from Eqs. (30a) and (32b) do not restrict the parameters, since they are always satisfied for $\mu < 0$. The same is also valid for the bound on the lightest Higgs boson mass, Eq. (33), due to the heavy SUSY spectrum.

6 The Deviation from YU

The deviation from YU is estimated by employing Eq. (27). In the allowed (shaded) area of Fig. 5 (for $\mu > 0$) which corresponds to the central value of $m_b(M_Z)$ in Eq. (1), the ranges of the parameters c , δh_τ , δh_b and $\tan \beta$ are

$$0.14 \lesssim c \lesssim 0.17, \quad 0.24 \lesssim \delta h_\tau = -\delta h_b \lesssim 0.29 \quad \text{and} \quad 58 \lesssim \tan \beta \lesssim 59.$$

However, letting $m_b(M_Z)$ vary in its 95% c.l. range in Eq. (1), we find that, in the corresponding allowed area, these parameters range as follows:

$$0.11 \lesssim c \lesssim 0.19, \quad 0.2 \lesssim \delta h_\tau = -\delta h_b \lesssim 0.32 \quad \text{and} \quad 57 \lesssim \tan \beta \lesssim 60.$$

In the lightly shaded area of Fig. 8 (for $\mu < 0$), which is obtained by allowing $m_b(M_Z)$ to vary in the range of Eq. (1), the parameters above range as follows:

$$0.01 \lesssim -c \lesssim 0.06, \quad 0.04 \lesssim -\delta h_\tau \lesssim 0.23, \quad \delta h_b = 0 \quad \text{and} \quad 46 \lesssim \tan \beta \lesssim 49.$$

For $m_b(M_Z) \simeq 2.888$ GeV, in the corresponding allowed area, these ranges become

$$0.036 \lesssim -c \lesssim 0.045, \quad 0.14 \lesssim -\delta h_\tau \lesssim 0.17, \quad \delta h_b = 0 \quad \text{and} \quad 47 \lesssim \tan \beta \lesssim 48.$$

We observe that, as we increase [decrease] $m_b(M_Z)$ for $\mu > 0$ [$\mu < 0$], the parameter $|c|$ decreases and we get closer to exact YU. This behavior is certainly consistent with the fact (see also Sec. 1) that the value of $m_b(M_Z)$ which corresponds to exact YU lies well above [a little below] its 95% c.l. range for $\mu > 0$ [$\mu < 0$].

Note, finally, that, for $\mu > 0$, the required deviation from YU is not so small. In spite of this, the restrictions from YU are not completely lost but only somewhat weakened. In particular, $\tan \beta$ remains large and close to 60. Actually, our model is much closer to YU than generic models where the Yukawa coupling constants can differ even by orders of magnitude. Also, the deviation from YU is generated here in a natural, systematic, controlled and well-motivated way.

7 Direct Detection of Neutralinos

As we showed in Sec. 5.1, our $\mu > 0$ model possesses a wide and natural range of parameters allowed by all the relevant astrophysical and experimental constraints. It would be, thus, interesting to investigate whether the predicted LSPs in the universe could be detected in the current or planned experiments. This can be done by first calculating the elastic scattering of the LSPs with nuclei [44, 60]. To accomplish this goal, we need an effective Lagrangian (see Sec. A.2) derived from the MSSM Lagrangian (see Sec. A.1) and providing a reliable description of the neutralino–quark interaction. We also need a procedure for going from the quark to the nucleon level (see Sec. 7.1) and from the nucleon to the nucleus (see Secs. 7.2, A.3 and A.4).

7.1 Scalar Neutralino–Proton Cross Section

The quantity which is being conventionally used in the recent literature (see e.g. Refs. [61, 62, 63]) for comparing experimental [64, 65, 66] and theoretical results is the spin independent (SI) neutralino–proton ($\tilde{\chi} - p$) cross section (at zero momentum transfer) $\sigma_{\tilde{\chi}p}^{\text{SI}}$ calculated by applying Eq. (A.24) with $A_N = Z_N = 1$. The SI effective $\tilde{\chi} - p$ coupling f_p is calculated using the full one-loop treatment of Refs. [67, 68] (already used in Ref. [16]), which, however, agrees with the tree-level approximation (see Eq. (A.25)) for the values of the SUSY parameters encountered in our model. The values in Eq. (A.26) [62] were adopted for the renormalization-invariant functions $f_{T_q}^p$ (with $q = u, d, s$) needed for the calculation of f_p .

Combining the sensitivities of the recent [64] and planned [65] experiments, we obtain the following observationally interesting region:

$$\text{a)} \quad 3 \times 10^{-9} \text{ pb} \lesssim \sigma_{\tilde{\chi}p}^{\text{SI}} \quad \text{and} \quad \text{b)} \quad \sigma_{\tilde{\chi}p}^{\text{SI}} \lesssim 2 \times 10^{-6} \text{ pb}, \quad (37)$$

for $150 \text{ GeV} \lesssim m_{\text{LSP}} \lesssim 500 \text{ GeV}$. For the allowed values of the SUSY parameters of our model, $\sigma_{\tilde{\chi}p}^{\text{SI}}$ lies beyond the preferred range of DAMA [66], $(1 - 10) \times 10^{-6} \text{ pb}$, which though has mostly been excluded by other collaborations (e.g. EDELWEISS and ZEPLIN I [64]).

Allowing $\Omega_{\text{LSP}} h^2$ and the hadronic inputs $f_{T_q}^p$ to vary within their ranges in Eqs. (28) and (A.26) respectively, we derive the shaded band on the $m_{\text{LSP}} - \sigma_{\tilde{\chi}p}^{\text{SI}}$ plane (Fig. 9). The bold solid line corresponds to the central values of $\Omega_{\text{LSP}} h^2$ and $f_{T_q}^p$. Note that the width of the band is almost exclusively due to the variation of $f_{T_q}^p$ since, for fixed m_{LSP} , $\sigma_{\tilde{\chi}p}^{\text{SI}}$ is almost insensitive to the variation of $\Omega_{\text{LSP}} h^2$ within the range of Eq. (28) (or, equivalently, to the required variation of $\Delta_{\tilde{\chi}_2}$). We observe that, for the allowed m_{LSP} 's, there are $\sigma_{\tilde{\chi}p}^{\text{SI}}$'s which lie within the margin of Eq. (37). Therefore, the LSPs predicted by our model can be detectable in the near future experiments. In particular, employing central values for $\Omega_{\text{LSP}} h^2$ and $f_{T_q}^p$, we find

$$5 \times 10^{-7} \text{ pb} \gtrsim \sigma_{\tilde{\chi}p}^{\text{SI}} \gtrsim 3 \times 10^{-9} \text{ pb} \quad \text{for } 179.7 \text{ GeV} \lesssim m_{\text{LSP}} \lesssim 300 \text{ GeV}. \quad (38)$$

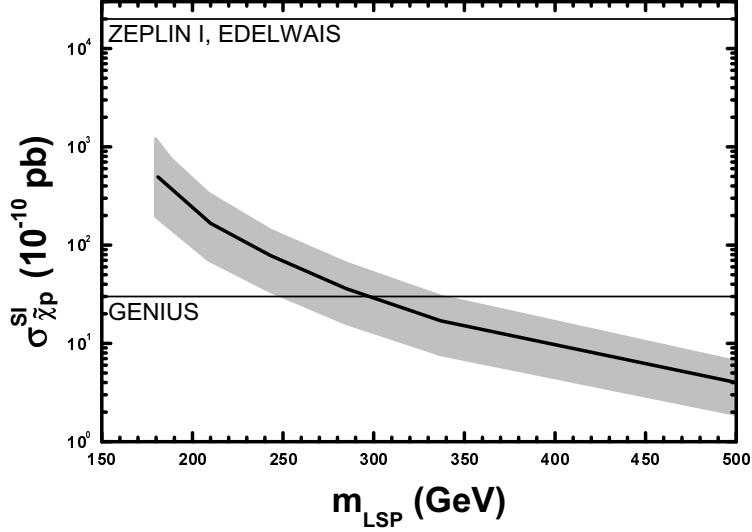


FIGURE 9: The SI $\tilde{\chi} - p$ cross section $\sigma_{\tilde{\chi}p}^{\text{SI}}$ versus m_{LSP} for $\mu > 0$ and $m_b(M_Z) = 2.888$ GeV. The bold solid line is derived by fixing $\Omega_{\text{LSP}} h^2$ and $f_{T_q}^p$ to their central values in Eqs. (28) and (A.26) respectively, whereas the shaded band by allowing $\Omega_{\text{LSP}} h^2$ and $f_{T_q}^p$ to vary in their ranges in these equations. The region of Eq. (37), which is preferred by the various experimental projects, is approximately limited between the two thin solid lines.

These values are somewhat higher than the ones obtained in similar estimations (see e.g. the third paper in Ref. [34]) with lower $\tan \beta$'s. Furthermore, the upper bound on m_{LSP} in Eq. (34) implies a lower bound on $\sigma_{\tilde{\chi}p}^{\text{SI}}$. Namely,

$$\sigma_{\tilde{\chi}p}^{\text{SI}} \gtrsim 1.6 \text{ (0.8)} \times 10^{-10} \text{ pb}, \quad (39)$$

where the bound in parenthesis is derived by allowing $f_{T_q}^p$ to vary.

7.2 Detection Rate of Neutralinos

The total detection rate (events per day) of LSPs per kgr of detector material (consisting of nuclei N) can be found by [68, 69]

$$R_{\tilde{\chi}}(N) = \frac{\rho_{\tilde{\chi}}^0}{\sqrt{\pi} v_0 m_{\tilde{\chi}} \mu_{\tilde{\chi}N}} \int_{Q_T}^{\infty} dQ_r \left(\sigma_{\tilde{\chi}N}^{\text{SI}} F^2(Q_r) + \sigma_{\tilde{\chi}N}^{\text{SD}} \frac{S(Q_r)}{S(0)} \right) T(Q_r). \quad (40)$$

Here Q_r is the (recoil) energy transferred to the nucleus, Q_T is the detector threshold energy below which the detector is insensitive to LSP–nucleus recoils, $\mu_{\tilde{\chi}N}$ is the reduced mass (evaluated in Eq. (A.24), $\sigma_{\tilde{\chi}N}^{\text{SI [SD]}}$ is the SI [spin dependent (SD)]

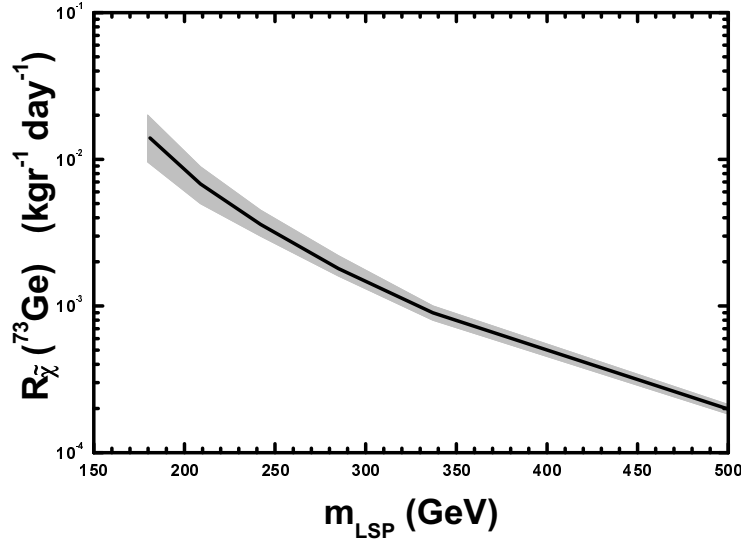


FIGURE 10: The LSP detection rate $R_{\tilde{\chi}}(^{73}\text{Ge})$ for a ^{73}Ge detector versus m_{LSP} for $\mu > 0$ and $m_b(M_Z) = 2.888$ GeV. The solid line is derived by fixing $\Omega_{\text{LSP}}h^2$, $f_{T_q}^{p[n]}$ and $\Delta_q^{p[n]}$ to their central values in Eqs. (28), (A.26) [(A.27)] and (A.30) [(A.29)] respectively, whereas the shaded band by allowing $\Omega_{\text{LSP}}h^2$, $f_{T_q}^{p[n]}$ and $\Delta_q^{p[n]}$ to vary in their ranges in these equations.

$\tilde{\chi} - \text{N}$ cross section (evaluated in Eq. (A.24) [Eq. (A.28)]) at zero Q_r , $\rho_{\tilde{\chi}}^0$ is the total local CDM density and v_0 is the circular velocity of the sun w.r.t. the galactic rest frame. Given the significant uncertainties involved in the determination of the two last quantities, we adopt their most popular values 0.3 GeV/cm 3 and 220 km/sec respectively. The derivation of the SI and SD form factors $F(Q_r)$ and $S(Q_r)/S(0)$ is also subject to considerable uncertainty. They are determined by closely following the analysis of Ref. [69] (and Ref. [68]). There, we can also find the function $T(Q_r)$ which depends on the minimal velocity of the incident LSPs and the velocity of earth (w.r.t. the galactic rest frame), which generates an annual modulation [70].

In Fig. 10, we display $R_{\tilde{\chi}}(^{73}\text{Ge})$ as a function m_{LSP} for $Q_T = 11$ keV and for the second of June. The shaded region is derived by allowing $\Omega_{\text{LSP}}h^2$, $f_{T_q}^{p[n]}$ and $\Delta_q^{p[n]}$ (see Secs. A.3 and A.4) to vary within their ranges in Eqs. (28), (A.26) [(A.27)] and (A.30) [(A.29)] respectively, whereas the solid line by fixing them to their central values. Note that the width of the band is almost exclusively due to the variation of $\sigma_{\tilde{\chi}\text{N}}^{\text{SI}}$, since $\sigma_{\tilde{\chi}\text{N}}^{\text{SD}}$ is almost insensitive to the aforementioned variations and an order of magnitude smaller than $\sigma_{\tilde{\chi}\text{N}}^{\text{SI}}$. The resulting $R_{\tilde{\chi}}(^{73}\text{Ge})$ is a little lower than the one obtained with the naive choice $F(Q_r) = S(Q_r)/S(0) = 1$ and significantly lower than the one corresponding to a wino or Higgsino LSP (compare with Ref. [71]).

8 A Resolution of the μ Problem

An important shortcoming of MSSM is that there is no understanding of how the SUSY μ term, with the right magnitude of $|\mu| \sim 10^2 - 10^3$ GeV, arises. One way [23] to solve this μ problem is via a PQ symmetry $U(1)_{\text{PQ}}$ [24], which also solves the strong CP problem. This solution is based on the observation [72] that the axion decay constant f_a , which is the symmetry breaking scale of $U(1)_{\text{PQ}}$, is (normally) intermediate ($\sim 10^{11} - 10^{12}$ GeV) and, thus, $|\mu| \sim f_a^2/M_S$. The scale f_a is, in turn, $\sim (m_{3/2} M_S)^{1/2}$, where $m_{3/2} \sim 1$ TeV is the gravity-mediated soft SUSY breaking scale (gravitino mass). In order to implement this solution of the μ problem, we introduce [23] a pair of superfields N and \bar{N} (see Table 1) with the following non-renormalizable couplings in the superpotential [73]:

$$W_{\text{PQ}} = \lambda_\mu \frac{N^2 h^2}{M_S} + \lambda'_\mu \frac{N^2 h'^2}{M_S} + \lambda \frac{N^2 H^c \bar{H}^c h' h}{M_S^3} + \lambda_{\text{PQ}} \frac{N^2 \bar{N}^2}{M_S}. \quad (41)$$

Here, λ_μ , λ'_μ , λ and λ_{PQ} are taken positive by redefining the phases of N and \bar{N} . After SUSY breaking, the $N^2 \bar{N}^2$ term leads to the scalar potential

$$\begin{aligned} V_{\text{PQ}} = & \left(m_{3/2}^2 + 4\lambda_{\text{PQ}}^2 \left| \frac{N \bar{N}}{M_S} \right|^2 \right) [(|N| - |\bar{N}|)^2 + 2|N||\bar{N}|] \\ & + 2|A|m_{3/2}\lambda_{\text{PQ}} \frac{|N \bar{N}|^2}{M_S} \cos(\epsilon + 2\theta + 2\bar{\theta}), \end{aligned} \quad (42)$$

where A is the dimensionless coefficient of the soft SUSY breaking term corresponding to the superpotential term $N^2 \bar{N}^2$ and $\epsilon, \theta, \bar{\theta}$ are the phases of A, N, \bar{N} respectively. Minimization of V_{PQ} then requires $|N| = |\bar{N}|$, $\epsilon + 2\theta + 2\bar{\theta} = \pi$ and V_{PQ} takes the form

$$V_{\text{PQ}} = 2|N|^2 m_{3/2}^2 \left(4\lambda_{\text{PQ}}^2 \frac{|N|^4}{m_{3/2}^2 M_S^2} - |A|\lambda_{\text{PQ}} \frac{|N|^2}{m_{3/2} M_S} + 1 \right). \quad (43)$$

For $|A| > 4$, the absolute minimum of the potential is at

$$|\langle N \rangle| = |\langle \bar{N} \rangle| \equiv \frac{f_a}{2} = \sqrt{m_{3/2} M_S} \sqrt{\frac{|A| + \sqrt{|A|^2 - 12}}{12\lambda_{\text{PQ}}}} \sim \sqrt{m_{3/2} M_S}. \quad (44)$$

The μ term is generated predominantly via the terms $N^2 h^2$ and $N^2 h'^2$ of Eq. (41) with $|\mu| \sim |\langle N \rangle|^2/M_S$, which is of the right magnitude.

The potential V_{PQ} also has a local minimum at $N = \bar{N} = 0$, which is separated from the global PQ minimum by a sizable potential barrier preventing a successful transition from the trivial to the PQ vacuum. This situation persists at all cosmic temperatures after reheating, as has been shown [27] by considering the one-loop temperature corrections [74] to the scalar potential. We are, thus, obliged to assume that, after the termination of inflation, the system emerges with the appropriate combination of initial conditions so that it is led [75] to the PQ vacuum.

9 Proton Stability

We can assign baryon number $1/3$ [$-1/3$] to all color triplets [antitriplets]. Recall that there are (anti)triplets not only in F, F^c but also in H^c, \bar{H}^c, G . Lepton number is then defined via $B - L$. Before the inclusion of the extra Higgs superfields (see Table 1), B (and L) violation comes from the following terms [27]

$$F^c F^c H^c H^c, \quad FF\bar{H}^c \bar{H}^c hh, \quad FF\bar{H}^c \bar{H}^c \bar{N}^2 \quad (45)$$

(and terms containing the combinations $(H^c)^4$, $(\bar{H}^c)^4$), which give couplings like $u^c d^c d_H^c \nu_H^c$ (or $u^c d^c u_H^c e_H^c$), $u d \bar{d}_H^c \bar{\nu}_H^c$ (or $u d \bar{u}_H^c \bar{e}_H^c$) with appropriate coefficients. Also, the terms $GH^c H^c$ and $G\bar{H}^c \bar{H}^c$ give rise to the B (and L) violating couplings $g^c u_H^c d_H^c$, $\bar{g}^c \bar{u}_H^c \bar{d}_H^c$. All other combinations are B (and L) conserving since all their $SU(4)_c$ **4**'s are contracted with $\bar{\mathbf{4}}$'s.

The dominant contribution to proton decay comes from effective dimension five operators generated by one-loop diagrams with two of the u_H^c, d_H^c or one of the u_H^c, d_H^c and one of the ν_H^c, e_H^c circulating in the loop. The amplitudes corresponding to these operators are estimated to be at most of order $m_{3/2} M_{\text{GUT}}/M_S^3 \lesssim 10^{-34} \text{ GeV}^{-1}$. This makes the proton practically stable.

After the inclusion of the superfields h' and \bar{h}' , the couplings

$$FF\bar{H}^c \bar{H}^c hh', \quad FF\bar{H}^c \bar{H}^c h' h' \quad (46)$$

(as well as the new couplings containing arbitrary powers of the combinations $(H^c)^4$, $(\bar{H}^c)^4$) give rise [9] to additional B and L number violation. However, their contribution to proton decay is subdominant to the one arising from the terms of Eq. (45). One can further show [9] that the inclusion of the superfields ϕ and $\bar{\phi}$ also gives a subdominant contribution to the proton decay.

10 The Inflationary Scenario

One of the most promising inflationary scenarios is hybrid inflation [76], which uses two real scalars: one which provides the vacuum energy density for inflation and a second which is the slowly varying field during inflation. This scheme is naturally incorporated [77] in SUSY GUTs (for an updated review, see Ref. [78]), but in its standard realization has the following problem [79]: if the GUT gauge symmetry breaking predicts monopoles (and this is the case of G_{PS} which predicts doubly charged monopoles [80]), they are copiously produced at the end of inflation leading to a cosmological catastrophe [81]. One way to remedy this is to generate a shifted inflationary trajectory so that G_{PS} is already broken during inflation. This could be achieved [27] in our SUSY GUT model even before the introduction of the extra Higgs superfields (see Table 1), but only by utilizing non-renormalizable terms. The inclusion of h' and \bar{h}' does not change this situation, which thus also holds in our

$\mu < 0$ model. This model is though excluded by imposing the restrictions of Sec. 4. On the other hand, for $\mu > 0$, the inclusion of ϕ and $\bar{\phi}$ very naturally gives rise [25] to a shifted path, but only with renormalizable interactions (for similar recent analyses in the context of a $SU(5)$ SUSY GUT, see Ref. [82]).

10.1 The Shifted Inflationary Path

As we showed in Sec. 2.2, the deviation from YU which is needed for $\mu > 0$ can be achieved by the inclusion of the superfields $\phi, \bar{\phi}$. In the presence of these superfields, a new version [25] of shifted hybrid inflation [27] can take place, without invoking any non-renormalizable superpotential terms.

Indeed, these fields lead to three new renormalizable terms in the part of the superpotential which is relevant for inflation. This is given by

$$W = \kappa S(H^c \bar{H}^c - M^2) - \beta S\phi^2 + m\phi\bar{\phi} + \lambda\bar{\phi}H^c\bar{H}^c, \quad (47)$$

where $M, m \sim M_{\text{GUT}}$, and κ, β and λ are dimensionless coupling constants with $M, m, \kappa, \lambda > 0$ by field redefinitions. For simplicity, we take $\beta > 0$ (the parameters are normalized so that they correspond to the couplings between the SM singlet components of the superfields).

The scalar potential obtained from W is given by

$$\begin{aligned} V = & |\kappa(H^c \bar{H}^c - M^2) - \beta\phi^2|^2 + |2\beta S\phi - m\bar{\phi}|^2 + |m\phi + \lambda H^c \bar{H}^c|^2 \\ & + |\kappa S + \lambda\bar{\phi}|^2 (|H^c|^2 + |\bar{H}^c|^2) + \text{D-terms}. \end{aligned} \quad (48)$$

Vanishing of the D-terms yields $\bar{H}^c * = e^{i\vartheta} H^c$ (H^c, \bar{H}^c lie in the $\nu_H^c, \bar{\nu}_H^c$ direction). We restrict ourselves to the direction with $\vartheta = 0$ which contains the shifted inflationary path and the SUSY vacua (see below). Performing appropriate R and gauge transformations, we bring H^c, \bar{H}^c and S to the positive real axis.

From the potential in Eq. (48), we find that the SUSY vacuum lies at

$$\frac{H^c \bar{H}^c}{M^2} \equiv \left(\frac{v_0}{M}\right)^2 = \frac{1}{2\xi} \left(1 - \sqrt{1 - 4\xi}\right), \quad \frac{\phi}{M} = -\sqrt{\frac{\kappa\xi}{\beta}} \left(\frac{v_0}{M}\right)^2 \quad (49)$$

with $S = 0$ and $\bar{\phi} = 0$, where $\xi = \beta\lambda^2 M^2 / \kappa m^2 < 1/4$. The potential possesses a ‘shifted’ flat direction (besides the trivial one) at

$$\frac{H^c \bar{H}^c}{M^2} \equiv \left(\frac{v}{M}\right)^2 = \frac{2\kappa^2(\frac{1}{4\xi} + 1) + \frac{\lambda^2}{\xi}}{2(\kappa^2 + \lambda^2)}, \quad \frac{\phi}{M} = -\frac{1}{2} \sqrt{\frac{\kappa}{\beta\xi}}, \quad \bar{\phi} = -\frac{\kappa}{\lambda} S \quad (50)$$

with $S > 0$ and a constant potential energy density V_0 given by

$$\frac{V_0}{M^4} = \frac{\kappa^2\lambda^2}{\kappa^2 + \lambda^2} \left(\frac{1}{4\xi} - 1\right)^2, \quad (51)$$

which can be used as inflationary path. $V_0 \neq 0$ breaks SUSY on this path, while the constant non-zero values of H^c , \bar{H}^c break the GUT gauge symmetry too. The SUSY breaking implies the existence of one-loop radiative corrections [83] which lift the classical flatness of this path yielding the necessary inclination for driving the inflaton towards the SUSY vacuum.

The one-loop radiative corrections to V along the shifted inflationary trajectory are calculated by using the Coleman-Weinberg formula [84]:

$$\Delta V = \frac{1}{64\pi^2} \sum_i (-)^{F_i} M_i^4 \ln \frac{M_i^2}{\Lambda^2}, \quad (52)$$

where the sum extends over all helicity states i , F_i and M_i^2 are the fermion number and mass squared of the i th state and Λ is a renormalization mass scale. In order to use this formula for creating a logarithmic slope which drives the canonically normalized real inflaton field $\sigma = \sqrt{2(\kappa^2 + \lambda^2)}S/\lambda$ towards the minimum, one has first to derive the mass spectrum of the model on the shifted inflationary path. This is a quite complicated task and we will skip it here.

10.2 Inflationary Observables

The slow roll parameters are given by (see e.g. Ref. [85])

$$\epsilon \simeq \frac{m_P^2}{2} \left(\frac{V'(\sigma)}{V_0} \right)^2 \quad \text{and} \quad \eta \simeq m_P^2 \frac{V''(\sigma)}{V_0}, \quad (53)$$

where the primes denote derivation w.r.t. the real normalized inflaton field σ and $m_P \simeq 2.44 \times 10^{18}$ GeV is the reduced Planck scale. The conditions for inflation to take place are $\epsilon \leq 1$ and $|\eta| \leq 1$.

The number of e-foldings that our present horizon scale suffered during inflation can be calculated as follows (see e.g. Ref. [85]):

$$N_Q \simeq \frac{1}{m_P^2} \int_{\sigma_f}^{\sigma_Q} \frac{V_0}{V'(\sigma)} d\sigma \simeq \ln \left(4.41 \times 10^{11} T_r^{\frac{1}{3}} V_0^{\frac{1}{6}} \right), \quad (54)$$

where σ_f [σ_Q] is the value of σ at the end of inflation [when our present horizon scale crossed outside the inflationary horizon] and $T_r \simeq 10^9$ GeV is the reheat temperature taken to saturate the gravitino constraint [86].

The quadrupole anisotropy of the CMBR can be calculated as follows (see e.g. Ref. [85]):

$$\left(\frac{\delta T}{T} \right)_Q \simeq \frac{1}{12\sqrt{5}} \frac{\sqrt{V_0^3}}{m_P^3 V'(\sigma_Q)}. \quad (55)$$

Fixing $(\delta T/T)_Q \simeq 6.6 \times 10^{-6}$ to its central value from COBE [26] (under the condition that the spectral index $n = 1$), we can determine one of the free parameters

(say β) in terms of the others (m , κ and λ). For instance, one finds [25] $\beta = 0.1$ for $m = 4.35 \times 10^{15}$ GeV and $\kappa = \lambda = 3 \times 10^{-2}$. In this case, the instability point of the shifted path is at $\sigma_c \simeq 3.55 \times 10^{16}$ GeV, $\sigma_f \simeq 1.7 \times 10^{17}$ GeV and $\sigma_Q \simeq 1.6 \times 10^{18}$ GeV. Also, $M \simeq 2.66 \times 10^{16}$ GeV, $N_Q \simeq 57.7$ and the spectral index $n \simeq 0.98$. Note that the slow roll conditions are violated and inflation ends well before reaching the instability point at σ_c . We see that the COBE constraint can be easily satisfied with natural values of the parameters. Moreover, superheavy SM non-singlets with masses $\ll M_{\text{GUT}}$, which could disturb the unification of the MSSM gauge coupling constants, are not encountered.

10.3 SUGRA Corrections

As we emphasized, the new shifted hybrid inflation occurs at values of σ which are quite close to the reduced Planck scale. Thus, one cannot ignore the SUGRA corrections to the scalar potential.

The scalar potential in SUGRA, without the D-terms, is given by

$$V = e^{K/m_P^2} \left[(F_i)^* K^{i^* j} F_j - 3 \frac{|W|^2}{m_P^2} \right], \quad (56)$$

where K is the Kähler potential, $F_i = W_i + K_i W/m_P^2$, a subscript i [i^*] denotes derivation w.r.t. the complex scalar field ϕ^i [ϕ^{i^*}] and $K^{i^* j}$ is the inverse of the matrix $K_{j i^*}$.

Consider a (complex) inflaton Σ corresponding to a flat direction of global SUSY with $W_{i\Sigma} = 0$. We assume that the potential on this path depends only on $|\Sigma|$, which holds in our model due to a global symmetry. From Eq. (56), we find that the SUGRA corrections lift the flatness of the Σ direction by generating a mass squared for Σ (see e.g. Ref. [87])

$$m_\Sigma^2 = \frac{V_0}{m_P^2} - \frac{|W_\Sigma|^2}{m_P^2} + \sum_{i,j} (W_i)^* K_{\Sigma^* \Sigma}^{i^* j} W_j + \dots, \quad (57)$$

where the right hand side (RHS) is evaluated on the flat direction with the explicitly displayed terms taken at $\Sigma = 0$. The ellipsis represents higher order terms which are suppressed by powers of $|\Sigma|/m_P$. The slow roll parameter η then becomes

$$\eta = 1 - \frac{|W_\Sigma|^2}{V_0} + \frac{m_P^2}{V_0} \sum_{i,j} (W_i)^* K_{\Sigma^* \Sigma}^{i^* j} W_j + \dots, \quad (58)$$

which, in general, could be of order unity and, thus, invalidate [77, 88] inflation. This is the well-known η problem of inflation in local SUSY. Several proposals have been made to overcome this difficulty (for a review, see e.g. Ref. [87]).

In all versions of SUSY hybrid inflation, there is an automatic mutual cancellation between the first two terms in the RHS of Eq. (58). This is due to the fact that

$W_n = 0$ on the inflationary path for all field directions n which are perpendicular to this path, which implies that $|W_\Sigma|^2 = V_0$ on the path. This is an important feature since, in general, the sum of the first two terms in the RHS of Eq. (58) is positive and of order unity, thereby ruining inflation. Moreover, $W_n = 0$ also implies that the only contribution to the third term in the RHS of Eq. (58) comes from the term in K which is quartic in Σ . So the third term can be suppressed by mildly tuning just one parameter [89] and inflation could remain intact provided that the terms in the ellipsis can be ignored.

However, in our present model, inflation takes place at values of $|\Sigma|$ close to m_P . So, the terms in the ellipsis in the RHS of Eq. (58) cannot be ignored (in contrast to the case of the old version [27] of shifted hybrid inflation) and may easily invalidate inflation. We, thus, need to invoke here a mechanism which can ensure that the SUGRA corrections do not lift the flatness of the inflationary path to all orders. A suitable scheme has been suggested in Ref. [90]. It has been argued that special forms of the Kähler potential can lead to the cancellation of the SUGRA corrections which spoil slow roll inflation to all orders. In particular, a specific form of $K(\Sigma)$ (used in no-scale SUGRA models) was employed and a gauge singlet field Z with a similar $K(Z)$ was introduced. It was pointed out that, by assuming a superheavy VEV for the Z field through D-terms, an exact cancellation of the inflaton mass on the inflationary trajectory can be achieved.

The form of the Kähler potential for Σ used in Ref. [90] is given by

$$K(|\Sigma|^2) = -\mathcal{N}m_P^2 \ln \left(1 - \frac{|\Sigma|^2}{\mathcal{N}m_P^2} \right), \quad (59)$$

where $\mathcal{N} = 1$ or 2 ; here we will take $\mathcal{N} = 2$. In this case, the kinetic term of the real normalized inflaton field σ (note that $|\Sigma| = \sigma/\sqrt{2}$) is $(1/2)(\partial^2 K/\partial \Sigma \partial \Sigma^*)\dot{\sigma}^2$, where the overdot denotes derivation w.r.t. the cosmic time t and $\partial^2 K/\partial \Sigma \partial \Sigma^* = (1 - \sigma^2/2\mathcal{N}m_P^2)^{-2}$. Thus, the Lagrangian density on the shifted path is given by

$$\mathcal{L} = a^3(t) \left[\frac{1}{2}\dot{\sigma}^2 \left(1 - \frac{\sigma^2}{2\mathcal{N}m_P^2} \right)^{-2} - V(\sigma) \right], \quad (60)$$

where $a(t)$ is the scale factor of the universe.

The evolution equation of σ is found by varying this Lagrangian w.r.t. σ :

$$\left[\ddot{\sigma} + 3H\dot{\sigma} + \dot{\sigma}^2 \left(1 - \frac{\sigma^2}{2\mathcal{N}m_P^2} \right)^{-1} \frac{\sigma}{\mathcal{N}m_P^2} \right] \left(1 - \frac{\sigma^2}{2\mathcal{N}m_P^2} \right)^{-2} + V'(\sigma) = 0, \quad (61)$$

where H is the Hubble parameter. During inflation, the ‘friction’ term $3H\dot{\sigma}$ dominates over the other two terms in the brackets in Eq. (61). Thus, this equation reduces to the modified inflationary equation

$$\dot{\sigma} = -\frac{V'(\sigma)}{3H} \left(1 - \frac{\sigma^2}{2\mathcal{N}m_P^2} \right)^2. \quad (62)$$

Note that, for $\sigma \ll \sqrt{2\mathcal{N}}m_P$, this equation reduces to the standard inflationary equation.

To derive the slow roll conditions, we evaluate the sum of the first and the third term in the brackets in Eq. (61) by using Eq. (62):

$$\ddot{\sigma} + \dot{\sigma}^2 \left(1 - \frac{\sigma^2}{2\mathcal{N}m_P^2}\right)^{-1} \frac{\sigma}{\mathcal{N}m_P^2} = \frac{V'(\sigma)}{3H^2} H'(\sigma) \dot{\sigma} \left(1 - \frac{\sigma^2}{2\mathcal{N}m_P^2}\right)^2 - \frac{V''(\sigma)}{3H} \dot{\sigma} \left(1 - \frac{\sigma^2}{2\mathcal{N}m_P^2}\right)^2 + \frac{V'(\sigma)}{3H} \dot{\sigma} \left(1 - \frac{\sigma^2}{2\mathcal{N}m_P^2}\right) \frac{\sigma}{\mathcal{N}m_P^2}. \quad (63)$$

Comparing the first two terms in the RHS of Eq. (63) with $H\dot{\sigma}$, we obtain

$$\epsilon \simeq \frac{1}{2} m_P^2 \left(\frac{V'(\sigma)}{V_0}\right)^2 \left(1 - \frac{\sigma^2}{2\mathcal{N}m_P^2}\right)^2 \leq 1, \quad (64)$$

$$|\eta| \simeq m_P^2 \left|\frac{V''(\sigma)}{V_0}\right| \left(1 - \frac{\sigma^2}{2\mathcal{N}m_P^2}\right)^2 \leq 1. \quad (65)$$

The third term in the RHS of Eq. (63), compared to $H\dot{\sigma}$, yields $\sqrt{2}\sigma\epsilon^{1/2}/\mathcal{N}m_P \leq 1$, which is automatically satisfied provided that Eq. (64) holds and $\sigma \leq \mathcal{N}m_P/\sqrt{2}$. The latter is true for the values of σ which are relevant here. We see that the slow roll parameters ϵ and η now carry an extra factor $(1 - \sigma^2/2\mathcal{N}m_P^2)^2 \leq 1$. This leads, in general, to smaller σ_f 's. However, in our case, $\sigma_f \ll \sqrt{2\mathcal{N}}m_P$ (for $\mathcal{N} = 2$) and, thus, this factor is practically equal to unity. Consequently, its influence on σ_f is negligible.

The formulas for N_Q and $(\delta T/T)_Q$ are now also modified due to the presence of the extra factor $(1 - \sigma^2/2\mathcal{N}m_P^2)^2$ in Eq. (62). In particular, a factor $(1 - \sigma^2/2\mathcal{N}m_P^2)^{-2}$ must be included in the integrand in the RHS of Eq. (54) and a factor $(1 - \sigma_Q^2/2\mathcal{N}m_P^2)^{-4}$ in the RHS of Eq. (55). We find that, for the σ 's under consideration, these modifications have only a small influence on σ_Q if we use the same input values for the free parameters as in the global SUSY case. On the contrary, $(\delta T/T)_Q$ increases considerably. However, we can easily readjust the parameters so that the COBE requirements are again met. For instance, $(\delta T/T)_Q \simeq 6.6 \times 10^{-6}$ is now obtained [25] with $m = 3.8 \times 10^{15}$ GeV keeping $\kappa = \lambda = 3 \times 10^{-2}$, $\beta = 0.1$ as in global SUSY. In this case, $\sigma_c \simeq 2.7 \times 10^{16}$ GeV, $\sigma_f \simeq 1.8 \times 10^{17}$ GeV and $\sigma_Q \simeq 1.6 \times 10^{18}$ GeV. Also, $M \simeq 2.6 \times 10^{16}$ GeV, $N_Q \simeq 57.5$ and $n \simeq 0.99$.

11 Conclusions

We studied the CMSSM with $A_0 = 0$ applying a suitable set of YQUCs which originate from SUSY GUT models based on G_{PS} . For each sign of μ , an appropriate YQUC was chosen from this set so that an adequate deviation from YU which allows an acceptable $m_b(M_Z)$ is ensured. We, also, imposed the constraints from the CDM in the universe, $b \rightarrow s\gamma$, $\delta\alpha_\mu$ and m_h . We concluded that

- For $\mu > 0$, there exists a wide and natural range of CMSSM parameters which is consistent with all the above constraints. We found that $\tan \beta$ ranges between about 58 and 61 and the asymptotic splitting between the bottom (or tau) and the top Yukawa coupling constants varies in the range 26 – 35% for central values of $m_b(M_Z)$ and $\alpha_s(M_Z)$.
- For $\mu < 0$, despite the fact that, considering the τ -based calculation for α_μ^{SM} , the $\delta\alpha_\mu$ and CDM criteria can be simultaneously satisfied, the model is excluded since the $b \rightarrow s\gamma$ and CDM requirements remain incompatible. However, the deviation from YU needed for correcting $m_b(M_Z)$ is much smaller than in the previous case.

The predicted LSP mass in the $\mu > 0$ model can be as low as about 176 GeV with $\sigma_{\chi p}^{\text{SI}}$ in the range of the sensitivity of the planned direct CDM detectors, though with a low detection rate. Moreover, the $\mu > 0$ model resolves the μ problem of MSSM, predicts stable proton and gives rise to a new version of shifted hybrid inflation. The inflationary scenario relies on renormalizable terms only, can be consistent with the COBE constraint on the CMBR with natural values for the relevant parameters and avoids overproduction of monopoles at the end of inflation. Inflation takes place along a classically flat direction, where G_{PS} is spontaneously broken to G_{SM} . A readjustment of the input values of the free parameters is required after the introduction of a specific Kähler potential and an extra gauge singlet with a superheavy VEV via D-terms, which are to be included in order for the SUGRA corrections not to invalidate inflation.

Acknowledgments

We would like to thank M.E. Gómez, R. Jeannerot and S. Khalil for fruitful and pleasant collaborations from which parts of this work are culled. This research was supported by European Union under the RTN contracts HPRN-CT-2000-00148 and HPRN-CT-2000-00152.

Appendix A Neutralino–Nucleus Elastic Cross Section

In this Appendix, we sketch the derivation of the tree-level approximation $\sigma_{\tilde{\chi}N}^0$ to the total cross section at zero momentum transfer for the elastic scattering process $\tilde{\chi}N \rightarrow \tilde{\chi}N$ with N being a nucleus target. This quantity can be split into a scalar or SI ($\sigma_{\tilde{\chi}N}^{\text{SI}}$) and an axial-vector or SD ($\sigma_{\tilde{\chi}N}^{\text{SD}}$) part [60, 61, 62, 67, 68]:

$$\sigma_{\tilde{\chi}N}^0 = \sigma_{\tilde{\chi}N}^{\text{SI}} + \sigma_{\tilde{\chi}N}^{\text{SD}}. \quad (\text{A.1})$$

In the following, we present the ingredients needed for the calculation of each part.

A.1 The Relevant MSSM Lagrangian

We present, in terms of mass eigenstates, all the Feynman rules which are necessary for studying the neutralino-quark elastic scattering process.

A.1.1 Neutralino–Squark–Quark Vertex (Ref. [91], Fig. 24)

The Lagrangian which describes the neutralino–squark–quark interaction is

$$\mathcal{L}_{\tilde{\chi}\tilde{q}q} = \sqrt{2}g t_W \bar{q} \sum_{i=1}^2 \left(g_{iL}^q P_L + g_{iR}^q P_R \right) \tilde{\chi} \tilde{q}_i + \text{h.c.}, \quad (\text{A.2})$$

where h.c. denotes the hermitian conjugate, $P_{L[R]} = (1 - [+] \gamma_5)/2$, q is a quark field, g is the $SU(2)_L$ gauge coupling constant and $t_W = \tan \theta_W$. Here, we considered general flavor-diagonal squark mixing and \tilde{q}_1 , \tilde{q}_2 are the squark mass eigenstates defined as follows:

$$\begin{pmatrix} \tilde{q}_1 \\ \tilde{q}_2 \end{pmatrix} = R_{\tilde{q}}^T \begin{pmatrix} \tilde{q}_L \\ \tilde{q}_R \end{pmatrix}, \quad \text{where } R_{\tilde{q}} = \begin{pmatrix} c_{\tilde{q}} & -s_{\tilde{q}} \\ s_{\tilde{q}} & c_{\tilde{q}} \end{pmatrix}, \quad (\text{A.3})$$

$s_{\tilde{q}} = \sin \theta_{\tilde{q}}$ and $c_{\tilde{q}} = \cos \theta_{\tilde{q}}$ with $\theta_{\tilde{q}}$ being the $\tilde{q}_L - \tilde{q}_R$ mixing angle. The coefficients g_{iL}^q and g_{iR}^q in the mass eigenstate basis are

$$g_{1L}^q = c_{\tilde{q}} g_{LL}^q + s_{\tilde{q}} g_{LR}^q, \quad g_{1R}^q = c_{\tilde{q}} g_{RL}^q + s_{\tilde{q}} g_{RR}^q, \quad (\text{A.4})$$

$$g_{2L}^q = -s_{\tilde{q}} g_{LL}^q + c_{\tilde{q}} g_{LR}^q, \quad g_{2R}^q = -s_{\tilde{q}} g_{RL}^q + c_{\tilde{q}} g_{RR}^q. \quad (\text{A.5})$$

The g_{LL}^q , g_{LR}^q , g_{RR}^q and g_{RL}^q coefficients for the up-type quarks u , c and t are

$$g_{LL}^u = -\frac{m_u}{2M_W s_{\beta} t_W} N_{14}^*, \quad g_{LR}^u = \frac{2}{3} (c_W N_{11}'^* - s_W N_{12}'^*), \quad (\text{A.6})$$

$$g_{RR}^u = -\frac{m_u}{2M_W s_{\beta} t_W} N_{14}, \quad g_{RL}^u = -\frac{2}{3} c_W N_{11}' - \left(\frac{1}{2} + \frac{2}{3} s_W^2 \right) \frac{N_{12}'}{s_W} \quad (\text{A.7})$$

and for the down-type quarks d , s and b are

$$g_{LL}^d = -\frac{m_d}{2M_W c_{\beta} t_W} N_{13}^*, \quad g_{LR}^d = -\frac{1}{3} (c_W N_{11}'^* - s_W N_{12}'^*), \quad (\text{A.8})$$

$$g_{RR}^d = -\frac{m_d}{2M_W c_{\beta} t_W} N_{13}, \quad g_{RL}^d = \frac{1}{3} c_W N_{11}' + \left(\frac{1}{2} - \frac{1}{3} s_W^2 \right) \frac{N_{12}'}{s_W}, \quad (\text{A.9})$$

where $s_W = \sin \theta_W$, $c_W = \cos \theta_W$, $s_{\beta} = \sin \beta$, $c_{\beta} = \cos \beta$, $m_{u[d]}$ are the masses of the up-type [down-type] quarks and N is the matrix which diagonalizes the neutralino mass matrix. Finally, N_{11}' and N_{12}' are defined as follows [91]:

$$\begin{pmatrix} N_{11}' \\ N_{12}' \end{pmatrix} = \begin{pmatrix} c_W & s_W \\ -s_W & c_W \end{pmatrix} \begin{pmatrix} N_{11} \\ N_{12} \end{pmatrix}. \quad (\text{A.10})$$

A.1.2 Z-boson–Quark–Quark Vertex (Ref. [92], Fig. 71)

The Lagrangian which describes the Z-boson–quark–quark interaction is

$$\mathcal{L}_{Zqq} = g_Z \bar{q} \gamma^\mu (R_q P_R + L_q P_L) q Z_\mu, \quad (\text{A.11})$$

where R_q and L_q for the up-type [down-type] quarks read

$$L_{u[d]} = -[+] \left(1 - [+] 2 \frac{2[-1]}{3} s_W^2 \right) \quad \text{and} \quad R_{u[d]} = -2 \frac{2[-1]}{3} s_W^2, \quad (\text{A.12})$$

and $g_Z = g/2c_W$.

A.1.3 Z-boson–Neutralino–Neutralino Vertex (Ref. [92], Fig. 75)

The Lagrangian which describes the Z-boson–neutralino–neutralino interaction is

$$\mathcal{L}_{Z\tilde{\chi}\tilde{\chi}} = g_{Z\tilde{\chi}\tilde{\chi}} \bar{\tilde{\chi}} \gamma^\mu \gamma_5 \tilde{\chi} Z_\mu, \quad \text{where} \quad g_{Z\tilde{\chi}\tilde{\chi}} = \frac{g_Z}{2} (|N_{13}|^2 - |N_{14}|^2). \quad (\text{A.13})$$

A.1.4 Higgs–Quark–Quark Vertex (Ref. [91], Fig. 7)

The Lagrangian which describes the Higgs–quark–quark interaction is

$$\mathcal{L}_{h,H,A \, qq} = \bar{q} (g_{hqq} h + g_{Hqq} H + i g_{Aqq} \gamma_5 A) q, \quad (\text{A.14})$$

where the g_{hqq} , g_{Hqq} and g_{Aqq} coefficients for the up- and down-type quarks are

$$g_{huu} = -\frac{g m_u c_\alpha}{2 M_W s_\beta}, \quad g_{hdd} = \frac{g m_d s_\alpha}{2 M_W c_\beta}, \quad (\text{A.15})$$

$$g_{Huu} = -\frac{g m_u s_\alpha}{2 M_W s_\beta}, \quad g_{Hdd} = -\frac{g m_d c_\alpha}{2 M_W c_\beta}, \quad (\text{A.16})$$

$$g_{Auu} = -\frac{g m_u}{2 M_W} \tan^{-1} \beta, \quad g_{Add} = -\frac{g m_d}{2 M_W} \tan \beta, \quad (\text{A.17})$$

where $c_\alpha = \cos \alpha$ and $s_\alpha = \sin \alpha$ with α being the Higgs mixing angle [91].

A.1.5 Higgs–Neutralino–Neutralino Vertex (Ref. [91], Fig. 21)

The Lagrangian which describes the Higgs–neutralino–neutralino interaction is

$$\mathcal{L}_{h,H,A \, \tilde{\chi}\tilde{\chi}} = \frac{1}{2} \bar{\tilde{\chi}} (g_{h\tilde{\chi}\tilde{\chi}} h + g_{H\tilde{\chi}\tilde{\chi}} H + i g_{A\tilde{\chi}\tilde{\chi}} \gamma_5 A) \tilde{\chi}, \quad (\text{A.18})$$

where

$$g_{h[H]\tilde{\chi}\tilde{\chi}} = g (s_\alpha [-c_\alpha] Q_{11} + c_\alpha [s_\alpha] S_{11}) \quad \text{and} \quad g_{A\tilde{\chi}\tilde{\chi}} = g (s_\beta Q_{11} - c_\beta S_{11}) \quad (\text{A.19})$$

with

$$Q_{11} = N_{13} (N_{12} - t_W N_{11}) \quad \text{and} \quad S_{11} = N_{14} (N_{12} - t_W N_{11}). \quad (\text{A.20})$$

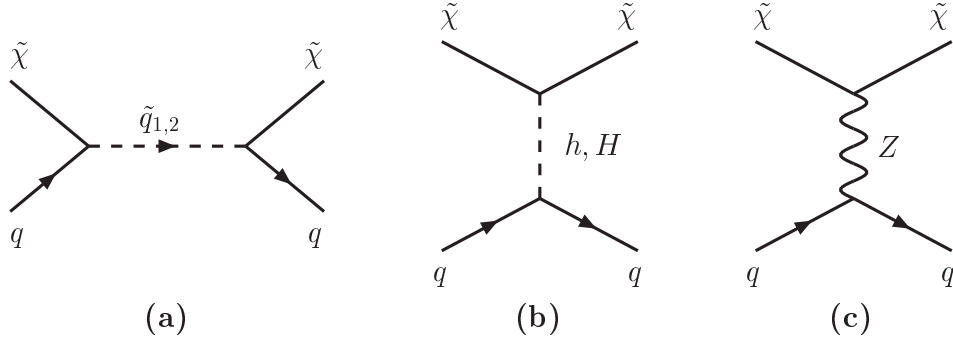


FIGURE 11: The five Feynman diagrams contributing to the neutralino–quark elastic scattering process $\tilde{\chi}q \rightarrow \tilde{\chi}q$: (a) the two diagrams with squark $\tilde{q}_{1,2}$ exchange, (b) the two diagrams with spin-0 neutral-Higgs-boson (h, H) exchange, and (c) the diagram with spin-1 Z -boson exchange.

A.2 Neutralino–Quark Effective Lagrangian

From the expressions above, it is possible [60, 67, 93], after the appropriate Fierz rearrangement, to derive the coefficients α_q^{SI} and α_q^{SD} contained in the effective four-fermion Lagrangian for the neutralino–quark elastic scattering:

$$\mathcal{L}_{\text{eff}} = \alpha_q^{\text{SI}} (\bar{\tilde{\chi}}\tilde{\chi}) (\bar{q}q) + \alpha_q^{\text{SD}} (\bar{\tilde{\chi}}\gamma^\mu\gamma_5\tilde{\chi}) (\bar{q}\gamma_\mu\gamma_5q) + \dots, \quad (\text{A.21})$$

where the ellipsis represents (i) terms (such as $\bar{\tilde{\chi}}\gamma_5\tilde{\chi}\bar{q}\gamma_5q$) which generate velocity-dependent and, thus, negligible [93] contributions to the elastic neutralino–quark cross section, (ii) loop corrections of order $m_{\tilde{q}_{1,2}}^{-4}$ which were previously considered in the literature [67] and can be safely neglected for $m_{\tilde{q}_{1,2}} \gg m_{\tilde{\chi}}$ [61, 62] (see below). The five tree-level Feynman diagrams contributing to the neutralino–quark scattering process are shown in Fig. 11. The s -channel squark-exchange diagrams contribute to both α_q^{SI} and α_q^{SD} , while the t -channel Higgs-exchange diagrams only to α_q^{SI} . The t -channel Z -exchange diagram contributes only to α_q^{SD} . These coefficients, in the non-relativistic limit, read

$$\alpha_q^{\text{SI}} = -g^2 t_W^2 \sum_{i=1,2} \frac{g_{iL}^q g_{iR}^q}{m_{\tilde{q}_i}^2 - (m_{\tilde{\chi}} + m_q)^2} + \frac{g_{h\tilde{\chi}\tilde{\chi}} g_{hqq}}{2m_h^2} + \frac{g_{H\tilde{\chi}\tilde{\chi}} g_{Hqq}}{2m_H^2}, \quad (\text{A.22})$$

$$\alpha_q^{\text{SD}} = -\frac{g^2 t_W^2}{2} \sum_{i=1,2} \frac{|g_{iL}^q|^2 + |g_{iR}^q|^2}{m_{\tilde{q}_i}^2 - (m_{\tilde{\chi}} + m_q)^2} - \frac{g_Z^2}{2M_Z^2} g_{Z\tilde{\chi}\tilde{\chi}} (R_q - L_q). \quad (\text{A.23})$$

Finally, let us note that, besides the neutralino–quark interaction in Eq. (A.21), there are also neutralino–gluon interactions with contributions arising from one-loop heavy quark and Higgs diagrams and the so-called twist-2 operators [67, 68]. However, these corrections are negligible for the values of SUSY parameters encountered in our $\mu > 0$ model (see Sec. 7).

A.3 Neutralino–Nucleus Spin Independent Cross Section

The SI part of $\sigma_{\tilde{\chi}N}^0$ can be parameterized as

$$\sigma_{\tilde{\chi}N}^{\text{SI}} = \frac{4}{\pi} \mu_{\tilde{\chi}N}^2 \left(Z_N f_p + (A_N - Z_N) f_n \right)^2, \quad \text{where } \mu_{\tilde{\chi}N} = \frac{m_{\tilde{\chi}} m_N}{m_{\tilde{\chi}} + m_N} \quad (\text{A.24})$$

is the neutralino–nucleus reduced mass and Z_N and A_N denote the atomic number and the mass number of the nucleus respectively. In the limit of $m_{\tilde{\chi}} \ll m_{\tilde{q}_{1,2}}$ (which is, in general, true unless \tilde{q}_2 is the next-to-LSP coinciding with the lightest stop [47, 94] or sbottom [16] quark) and $m_q \ll m_{\tilde{q}_{1,2}}$, the effective coupling $f_{p[n]}$ of the LSP to proton [neutron] is given by

$$f_{p[n]} = \sum_{q=u,d,s} \frac{m_{p[n]}}{m_q} f_{T_q}^{p[n]} \alpha_q^{\text{SI}} + \frac{2}{27} f_{T_G}^{p[n]} \sum_{q=c,b,t} \frac{m_{p[n]}}{m_q} \alpha_q^{\text{SI}} \quad (\text{A.25})$$

to lowest order in $m_{\tilde{q}_{1,2}}^{-1}$, where $m_{p[n]}$ is the proton [neutron] mass and the parameters $f_{T_q}^p$ and $f_{T_q}^n$ are taken to be [62]

$$f_{T_u}^p = 0.02 \pm 0.004, \quad f_{T_d}^p = 0.026 \pm 0.005, \quad f_{T_s}^p = 0.118 \pm 0.062, \quad (\text{A.26})$$

$$f_{T_u}^n = 0.014 \pm 0.003, \quad f_{T_d}^n = 0.036 \pm 0.008, \quad f_{T_s}^n = 0.118 \pm 0.062. \quad (\text{A.27})$$

with $f_{T_G}^{p[n]} = 1 - \sum_{q=u,d,s} f_{T_q}^{p[n]}$. In our numerical analysis, we use the running masses of b and t quark at the scale $m_{\tilde{\chi}}$.

A.4 Neutralino–Nucleus Spin Dependent Cross Section

The SD part of $\sigma_{\tilde{\chi}N}^0$ can be parameterized as follows:

$$\sigma_{\tilde{\chi}N}^{\text{SD}} = \frac{16}{\pi} \mu_{\tilde{\chi}N}^2 \Lambda^2 J_N (J_N + 1), \quad \text{where } \Lambda = \frac{1}{J_N} \left(\lambda_p \langle S_p \rangle + \lambda_n \langle S_n \rangle \right) \quad (\text{A.28})$$

and J_N is the total angular momentum of the nucleus ($9/2$ for ^{73}Ge). Also, $\langle S_{p[n]} \rangle$ is the expectation value of the spin content of the proton [neutron] group in the nucleus with explicit value, for a ^{73}Ge target, $\langle S_p \rangle_{^{73}\text{Ge}} = 0.011$ [$\langle S_n \rangle_{^{73}\text{Ge}} = 0.491$] in the shell model. Finally, the coefficient $\lambda_{p[n]}$ is parameterized in terms of the quark spin content of the proton [neutron] $\Delta_q^{p[n]}$ and the effective axial-vector couplings α_q^{SD} ($q = u, d, s$) as

$$\lambda_{p[n]} = \sum_{q=u,d,s} \alpha_q^{\text{SD}} \Delta_q^{p[n]}, \quad \text{where } \Delta_u^n = \Delta_d^p, \quad \Delta_d^n = \Delta_u^p \quad \text{and} \quad \Delta_s^n = \Delta_s^p \quad (\text{A.29})$$

with the factors Δ_q^p taken to be [62]

$$\Delta_u^p = +0.78 \pm 0.02, \quad \Delta_d^p = -0.48 \pm 0.02 \quad \text{and} \quad \Delta_s^p = -0.15 \pm 0.02. \quad (\text{A.30})$$

Needless to say that the formalism of this section remains valid even in the case of light stop [47, 94] or sbottom [16] quarks.

References

- [1] G.L. Kane, C. Kolda, L. Roszkowski and J.D. Wells, Phys. Rev. D **49**, 6173 (1994) [[hep-ph/9312272](#)].
- [2] G. Lazarides and C. Panagiotakopoulos, Phys. Lett. B **337**, 90 (1994) [[hep-ph/9403316](#)]; S. Khalil, G. Lazarides and C. Pallis, *ibid.* **508**, 327 (2001) [[hep-ph/0005021](#)].
- [3] B. Ananthanarayan, G. Lazarides and Q. Shafi, Phys. Rev. D **44**, 1613 (1991); Phys. Lett. B **300**, 245 (1993).
- [4] S. Raby, Rept. Prog. Phys. **67**, 755 (2004) [[hep-ph/0401155](#)].
- [5] L. Hall, R. Rattazzi and U. Sarid, Phys. Rev. D **50**, 7048 (1994) [[hep-ph/9306309](#)]; M. Carena, M. Olechowski, S. Pokorski and C.E.M. Wagner, Nucl. Phys. **B426**, 269 (1994) [[hep-ph/9402253](#)].
- [6] D. Pierce, J. Bagger, K. Matchev and R. Zhang, Nucl. Phys. **B491**, 3 (1997) [[hep-ph/9606211](#)].
- [7] M. Carena, D. Garcia, U. Nierste and C.E.M. Wagner, Nucl. Phys. **B577**, 88 (2000) [[hep-ph/9912516](#)].
- [8] S. Abel *et al.* (SUGRA Working Group Collaboration), [hep-ph/0003154](#).
- [9] M.E. Gómez, G. Lazarides and C. Pallis, Nucl. Phys. **B638**, 165 (2002) [[hep-ph/0203131](#)]; Phys. Rev. D **67**, 097701 (2003) [[hep-ph/0301064](#)].
- [10] C.T. Sachrajda, Nucl. Instrum. Meth. A **462**, 23 (2001) [[hep-lat/0101003](#)].
- [11] H. Baer, J. Ferrandis, K. Melnikov and X. Tata, Phys. Rev. D **66**, 074007 (2002) [[hep-ph/0207126](#)].
- [12] S.F. King and M. Oliveira, Phys. Rev. D **63**, 015010 (2001) [[hep-ph/0008183](#)].
- [13] T. Blažek, R. Dermíšek and S. Raby, Phys. Rev. Lett. **88**, 111804 (2002) [[hep-ph/0107097](#)]; Phys. Rev. D **65**, 115004 (2002) [[hep-ph/0201081](#)]; R. Dermíšek, S. Raby, L. Roszkowski and R. Ruiz de Austri, J. High Energy Phys. **04**, 037 (2003) [[hep-ph/0304101](#)].
- [14] D. Auto, H. Baer, C. Balázs, A. Belyaev, J. Ferrandis and X. Tata, J. High Energy Phys. **06**, 023 (2003) [[hep-ph/0302155](#)].
- [15] U. Chattopadhyay and P. Nath, Phys. Rev. D **65**, 075009 (2002) [[hep-ph/0110341](#)]; U. Chattopadhyay, A. Corsetti and P. Nath, *ibid.* **66**, 035003 (2002) [[hep-ph/0201001](#)].
- [16] C. Pallis, Nucl. Phys. **B678**, 398 (2004) [[hep-ph/0304047](#)].
- [17] G. Lazarides, Q. Shafi and C. Wetterich, Nucl. Phys. **B181**, 287 (1981); G. Lazarides and Q. Shafi, *ibid.* **B350**, 179 (1991).
- [18] D. Spergel *et al.*, Astrophys. J. Suppl. **148**, 175 (2003) [[astro-ph/0302209](#)].
- [19] For a review from the viewpoint of particle phycics, see A.B. Lahanas, N.E. Mavromatos and D.V. Nanopoulos, Int. J. Mod. Phys. D **12**, 1529 (2003) [[hep-ph/0308251](#)].
- [20] R. Barate *et al.* (ALEPH Collaboration), Phys. Lett. B **429**, 169 (1998); K. Abe *et al.* (BELLE Collaboration), *ibid.* **511**, 151 (2001) [[hep-ex/0103042](#)]; S. Chen *et al.* (CLEO Collaboration), Phys. Rev. Lett. **87**, 251807 (2001) [[hep-ex/0108032](#)].

- [21] G.W. Bennett *et al.* (Muon $g-2$ Collaboration), Phys. Rev. Lett. **89**, 101804 (2002); **89**, 129903(E) (2002) [[hep-ex/0208001](#)].
- [22] ALEPH, DELPHI, L3 and OPAL Collaborations, The LEP Higgs working group for Higgs boson searches, [hep-ex/0107029](#); LHWG-NOTE/2002-01, http://lephiggs.web.cern.ch/LEPHIGGS/papers/July2002_SM/index.html.
- [23] G. Lazarides and Q. Shafi, Phys. Rev. D **58**, 071702 (1998) [[hep-ph/9803397](#)].
- [24] R. Peccei and H. Quinn, Phys. Rev. Lett. **38**, 1440 (1977); S. Weinberg, *ibid.* **40**, 223 (1978); F. Wilczek, *ibid.* **40**, 279 (1978).
- [25] R. Jeannerot, S. Khalil and G. Lazarides, J. High Energy Phys. **07**, 069 (2002) [[hep-ph/0207244](#)].
- [26] C.L. Bennett *et al.*, Astrophys. J. **464**, L1 (1996) [[astro-ph/9601067](#)].
- [27] R. Jeannerot, S. Khalil, G. Lazarides and Q. Shafi, J. High Energy Phys. **10**, 012 (2000) [[hep-ph/0002151](#)].
- [28] G. Lazarides, in *Recent Developments in Particle Physics and Cosmology*, edited by G.C. Branco, Q. Shafi and J.I. Silva-Marcos (Kluwer Academic Publishers, Dordrecht, The Netherlands, 2001) p. 399 [[hep-ph/0011130](#)]; R. Jeannerot, S. Khalil and G. Lazarides, in *The Proceedings of Cairo International Conference on High Energy Physics*, edited by S. Khalil, Q. Shafi and H. Tallat (Rinton Press Inc., Princeton, 2001) p. 254 [[hep-ph/0106035](#)]; G. Lazarides and C. Pallis, [hep-ph/0404266](#) (to appear in the Proceedings of the BW2003 Workshop, Vrnjacka Banja, Serbia, 29 August-2 September 2003).
- [29] I. Antoniadis and G.K. Leontaris, Phys. Lett. B **216**, 333 (1989).
- [30] G. Lazarides, C. Panagiotakopoulos and Q. Shafi, Phys. Rev. Lett. **56**, 432 (1986).
- [31] N. Ganoulis, G. Lazarides and Q. Shafi, Nucl. Phys. **B323**, 374 (1989); G. Lazarides and Q. Shafi, *ibid.* **B329**, 182 (1990).
- [32] M.E. Gómez, G. Lazarides and C. Pallis, Phys. Rev. D **61**, 123512 (2000) [[hep-ph/9907261](#)]; Phys. Lett. B **487**, 313 (2000) [[hep-ph/0004028](#)].
- [33] M.E. Gómez and C. Pallis, [hep-ph/0303094](#) (published in the SUSY02 Proceedings).
- [34] J. Ellis, K.A. Olive, Y. Santoso and V.C. Spanos, Phys. Lett. B **565**, 176 (2003) [[hep-ph/0303043](#)]; H. Baer and C. Balázs, J. Cosmol. Astropart. Phys. **05**, 006 (2003) [[hep-ph/0303114](#)]; A.B. Lahanas and D.V. Nanopoulos, Phys. Lett. B **568**, 55 (2003) [[hep-ph/0303130](#)]; U. Chattopadhyay, A. Corsetti and P. Nath, Phys. Rev. D **68**, 035005 (2003) [[hep-ph/0303201](#)].
- [35] H. Goldberg, Phys. Rev. Lett. **50**, 1419 (1983); J.R. Ellis, J.S. Hagelin, D. V. Nanopoulos, K.A. Olive and M. Srednicki, Nucl. Phys. **B238**, 453 (1984).
- [36] See e.g. N. Fornengo, A. Riotto and S. Scopel, Phys. Rev. D **67**, 023514 (2003) [[hep-ph/0208072](#)]; C. Pallis, Astropart. Phys. **21**, 689 (2004) [[hep-ph/0402033](#)].
- [37] See also R. Allahverdi and M. Drees, Phys. Rev. Lett. **89**, 091302 (2002) [[hep-ph/0203118](#)]; Phys. Rev. D **66**, 063513 (2002) [[hep-ph/0205246](#)].
- [38] See e.g. M.S. Turner, Phys. Rev. D **33**, 889 (1986); Phys. Rep. **197**, 67 (1990).

- [39] See e.g. J. Ellis, K.A. Olive, Y. Santoso and V.C. Spanos, Phys. Lett. B **588**, 7 (2004) [[hep-ph/0312262](#)]; L. Covi, L. Roszkowski, R. Ruiz de Austri and M. Small, J. High Energy Phys. **06**, 003 (2004) [[hep-ph/0402240](#)].
- [40] G. Bélanger, F. Boudjema, A. Pukhov and A. Semenov, Comput. Phys. Commun. **149**, 103 (2002) [[hep-ph/0112278](#)].
- [41] G. Bélanger, F. Boudjema, A. Pukhov and A. Semenov, [hep-ph/0405253](#).
- [42] A. Djouadi, J. Kalinowski and M. Spira, Comput. Phys. Commun. **108**, 56 (1998) [[hep-ph/9704448](#)].
- [43] C. Pallis and M.E. Gómez, [hep-ph/0303098](#).
- [44] For recent reviews, see C. Muñoz, Int. J. Mod. Phys. A **19**, 3093 (2004) [[hep-ph/0309346](#)]; J.L. Feng, eConf. C0307282, **L11** (2003) [[hep-ph/0405215](#)].
- [45] A.B. Lahanas, D.V. Nanopoulos and V.C. Spanos, Phys. Rev. D **62**, 023515 (2000) [[hep-ph/9909497](#)]; J. Ellis, T. Falk, G. Ganis, K.A. Olive and M. Srednicki, Phys. Lett. B **510**, 236 (2001) [[hep-ph/0102098](#)].
- [46] J. Ellis, T. Falk, K.A. Olive and M. Srednicki, Astropart. Phys. **13**, 181 (2000); **15**, 413(E) (2001) [[hep-ph/9905481](#)].
- [47] J. Ellis, K. Olive and Y. Santoso, Astropart. Phys. **18**, 395 (2003) [[hep-ph/0112113](#)].
- [48] J. Edsjö, M. Schelke, P. Ullio and P. Gondolo, J. Cosmol. Astropart. Phys. **04**, 001 (2003) [[hep-ph/0301106](#)].
- [49] A.L. Kagan and M. Neubert, Eur. Phys. J. C **7**, 5 (1999) [[hep-ph/9805303](#)]; P. Gambino and M. Misiak, Nucl. Phys. **B611**, 338 (2001) [[hep-ph/0104034](#)].
- [50] M. Ciuchini, G. Degrassi, P. Gambino and G. Giudice, Nucl. Phys. **B527**, 21 (1998) [[hep-ph/9710335](#)].
- [51] G. Degrassi, P. Gambino and G.F. Giudice, J. High Energy Phys. **12**, 009 (2000) [[hep-ph/0009337](#)].
- [52] G. D'Ambrosio, G.F. Giudice, G. Isidori and A. Strumia, Nucl. Phys. **B645**, 155 (2002) [[hep-ph/0207036](#)].
- [53] S.P. Martin and J.D. Wells, Phys. Rev. D **64**, 035003 (2001) [[hep-ph/0103067](#)].
- [54] M. Davier, [hep-ex/0312065](#) (to appear in the SIGHAD03 Proceedings).
- [55] S.P. Martin and J.D. Wells, Phys. Rev. D **67**, 015002 (2003) [[hep-ph/0209309](#)].
- [56] K. Hagiwara, A.D. Martin, D. Nomura and T. Teubner, Phys. Lett. B **557**, 69 (2002) [[hep-ph/0209187](#)]; S. Narison, *ibid.* **568**, 231 (2003) [[hep-ph/0303004](#)].
- [57] S. Heinemeyer, W. Hollik and G. Weiglein, [hep-ph/0002213](#).
- [58] T. Nihei, L. Roszkowski and R. Ruiz de Austri, J. High Energy Phys. **05**, 063 (2001) [[hep-ph/0102308](#)].
- [59] T. Nihei, L. Roszkowski and R. Ruiz de Austri, J. High Energy Phys. **07**, 024 (2002) [[hep-ph/0206266](#)].

- [60] M.W. Goodman and E. Witten, Phys. Rev. D **31**, 3059 (1985); J. Ellis and R. Flores, Nucl. Phys. **B307**, 883 (1988); K. Griest, Phys. Rev. D **38**, 2357 (1988); **39**, 3802(E) (1989).
- [61] V. Bednyakov, H.V. Klapdor-Kleingrothaus and S. Kovalenko, Phys. Rev. D **50**, 7128 (1994) [[hep-ph/9401262](#)]; V. Bednyakov, H. Klapdor-Kleingrothaus, *ibid.* **63**, 095005 (2001) [[hep-ph/0011233](#)].
- [62] J. Ellis, A. Ferstl and K.A. Olive, Phys. Lett. B **481**, 304 (2000) [[hep-ph/0001005](#)]; *ibid.* **532**, 318 (2002) [[hep-ph/0111064](#)]; T. Nihei, L. Roszkowski and R. Ruiz de Austri, J. High Energy Phys. **12**, 034 (2002) [[hep-ph/0208069](#)]; H. Baer, C. Balázs, A. Belyaev and J. O'Farrill, J. Cosmol. Astropart. Phys. **09**, 007 (2003) [[hep-ph/0305191](#)].
- [63] M.E. Gómez and J.D. Vergados, Phys. Lett. B **512**, 252 (2001) [[hep-ph/0012020](#)]; D.G. Cerdeño, E. Gabrielli, M.E. Gómez and C. Muñoz, J. High Energy Phys. **06**, 030 (2003) [[hep-ph/0304115](#)]; D.G. Cerdeño and C. Muñoz, [hep-ph/0405057](#).
- [64] R. Abusaidi *et al.* (CDMS Collaboration), Phys. Rev. Lett. **84**, 5699 (2000) [[astro-ph/0002471](#)]; A. Benoit *et al.* (EDELWEISS Collaboration), Phys. Lett. B **545**, 43 (2002) [[hep-ph/0206271](#)].
- [65] H.V. Klapdor-Kleingrothaus *et al.* (GENIUS Colaboration), [hep-ph/9910205](#); H.V. Klapdor-Kleingrothaus, Nucl. Phys. B (Proc. Suppl.) **110**, 364 (2002) [[hep-ph/0206249](#)].
- [66] R. Bernabei *et al.* (DAMA Collaboration), Phys. Lett. B **480**, 23 (2000).
- [67] M. Drees and M. Nojiri, Phys. Rev. D **48**, 3483 (1993) [[hep-ph/9307208](#)].
- [68] G. Jungman, M. Kamionkowski and K. Griest, Phys. Rep. **267**, 195 (1996) [[hep-ph/9506380](#)]; <http://t8web.lanl.gov/people/jungman/neut-package.html>.
- [69] H. Baer and M. Brhlik, Phys. Rev. D **57**, 567 (1998) [[hep-ph/9706509](#)].
- [70] For an updated analysis, see J.D. Vergados, Phys. Rev. Lett. **83**, 3597 (1999); Phys. Rev D **67**, 103003 (2003) [[hep-ph/0303231](#)].
- [71] B. Murakami and J.D. Wells, Phys. Rev. D **64**, 015001 (2001) [[hep-ph/0011082](#)].
- [72] J.E. Kim and H.P. Nilles, Phys. Lett. B **138**, 150 (1984).
- [73] For an alternative class of superpotentials, see H. Murayama, H. Suzuki and T. Yanagida, Phys. Lett. B **291**, 418 (1992); K. Choi, E.J. Chun and J.E. Kim, *ibid.* **403**, 209 (1997) [[hep-ph/9608222](#)]; G. Lazarides and Q. Shafi, *ibid.* **489**, 194 (2000) [[hep-ph/0006202](#)]; E.J. Chun, K. Dimopoulos and D. Lyth, [hep-ph/0402059](#); A. Anisimov and M. Dine, [hep-ph/0405256](#).
- [74] L. Dolan and R. Jackiw, Phys. Rev. D **9**, 3320 (1974); S. Weinberg, *ibid.* **9**, 3357 (1974).
- [75] K. Dimopoulos, G. Lazarides, D. Lyth and R. Ruiz de Austri, J. High Energy Phys. **05**, 057 (2003) [[hep-ph/0303154](#)].
- [76] A.D. Linde, Phys. Rev. D **49**, 748 (1994) [[astro-ph/9307002](#)].
- [77] E.J. Copeland, A.R. Liddle, D.H. Lyth, E.D. Stewart and D. Wands, Phys. Rev. D **49**, 6410 (1994) [[astro-ph/9401011](#)].

- [78] V.N. Senoguz and Q. Shafi, Phys. Lett. B **567**, 79 (2003) [[hep-ph/0305089](#)]; *ibid.* **582**, 6 (2003) [[hep-ph/0309134](#)].
- [79] G. Lazarides and C. Panagiotakopoulos, Phys. Rev. D **52**, 559 (1995) [[hep-ph/9506325](#)].
- [80] G. Lazarides, M. Magg and Q. Shafi, Phys. Lett. B **97**, 87 (1980).
- [81] T.W.B. Kibble, J. Phys. A **9**, 387 (1976).
- [82] B. Kyae and Q. Shafi, J. High Energy Phys. **11**, 036 (2003) [[astro-ph/0302504](#)]; Phys. Lett. B **597**, 321 (2004) [[hep-ph/0404168](#)].
- [83] G. Dvali, R. Schaefer and Q. Shafi, Phys. Rev. D **73**, 1886 (1994) [[hep-ph/9406319](#)].
- [84] S. Coleman and E. Weinberg, Phys. Rev. D **7**, 1888 (1973).
- [85] G. Lazarides, Lect. Notes Phys. **592**, 351 (2002) [[hep-ph/0111328](#)]; [hep-ph/0204294](#).
- [86] M.Yu. Khlopov and A.D. Linde, Phys. Lett. B **138**, 265 (1984); J. Ellis, J.E. Kim and D.V. Nanopoulos, *ibid.* **145**, 181 (1984).
- [87] D.H. Lyth and A. Riotto, Phys. Rep. **314**, 1 (1999) [[hep-ph/9807278](#)].
- [88] E.D. Stewart, Phys. Rev. D **51**, 6847 (1995) [[hep-ph/9405389](#)].
- [89] G. Lazarides, R.K. Schaefer and Q. Shafi, Phys. Rev. D **56**, 1324 (1997) [[hep-ph/9608256](#)].
- [90] C. Panagiotakopoulos, Phys. Lett. B **459**, 473 (1999) [[hep-ph/9904284](#)].
- [91] J.F. Gunion and H.E. Haber, Nucl. Phys. **B272**, 1 (1986); **B402**, 567(E) (1993).
- [92] H.E. Haber and G.L. Kane, Phys. Rep. **117**, 75 (1985).
- [93] U. Chattopadhyay, T. Ibrahim and P. Nath, Phys. Rev. D **60**, 063505 (1999) [[hep-ph/9811362](#)]; T. Falk, A. Ferstl and K.A. Olive, Astropart. Phys. **13**, 301 (2000) [[hep-ph/9908311](#)].
- [94] C. Boehm, A. Djouadi and M. Drees, Phys. Rev. D **62**, 035012 (2000) [[hep-ph/9911496](#)].